

MATLAB SIMULATION OF SINGLE PHASE SHUNT ACTIVE POWER FILTER AND DEVELOPMENT OF EXPERIMENTAL SET UP

SHYAMSUNDAR JENA (110EE0199)



**Department of Electrical Engineering,
National Institute of Technology, Rourkela**

MATLAB SIMULATION OF SINGLE PHASE SHUNT ACTIVE POWER FILTER AND DEVELOPMENT OF EXPERIMENTAL SET UP

*A thesis submitted in partial fulfilment of the requirements for the degree of
Bachelor of Technology in “Electrical Engineering”*

By

SHYAMSUNDAR JENA (110EE0199)

Under the Supervision of

Prof. K.B.Mohanty



**Department of Electrical Engineering
National Institute of Technology
Rourkela-769008 (ODISHA)
May-2014**



DEPARTMENT OF ELECTRICAL ENGINEERING
NATIONAL INSTITUTE OF TECHNOLOGY, ROURKELA
ODISHA, INDIA-769008

CERTIFICATE

This is to certify that the thesis report titled "**MATLAB Simulation of Single Phase Shunt Active Power Filter and Development of Experimental Set up**", submitted to the National Institute of Technology, Rourkela by **Mr. Shyamsundar Jena, Roll No: 110EE0199** for the award of Bachelor of Technology in **Electrical Engineering** is a bona fide record of research work carried out by him under my supervision and guidance.

The candidate has fulfilled all the prescribed requirements.

The thesis report which is based on candidate's own work has not been submitted elsewhere for a degree/diploma.

In my opinion, the thesis report is of standard required for the award of a Bachelor of Technology in Electrical Engineering.

Prof. K.B. Mohanty

Supervisor

Department of Electrical Engineering

National Institute of Technology

Rourkela – 769 008 (ODISHA)

ACKNOWLEDGEMENTS

Fore mostly, I would like to express my sincere gratitude to my supervisor Prof. K.B. Mohanty, for his patience, motivation and financial support for the project work. I sincerely appreciate and value his esteem guidance and encouragement from the beginning till the end of my thesis.

I wish to express my sincere gratitude to Prof.A.K Panda (HOD) for approving the budget to purchase some of the components required for the project work. I am very much thankful to Mr.Maheswar Mahato, and Gobardhan Rana for assisting me in developing the experimental setup.

I would also like to thank Prof. P.K Ray, Prof. B.Chitti Babu, Prof. Gopalkrishna and other faculty members of Electrical Engineering Department, NIT Rourkela for their encouragement, support and motivation.

Last but not the least; I would also like to thank my parents, sister, brother and all well-wishers for their co-operation, sacrifice and motivational moral support which bring me to this level.

Shyamsundar Jena

DEDICATED TO
ALMIGHTY...

ABSTRACT

This project work presents a single phase shunt active power filter based on synchronous detection method. Due to wide use of nonlinear single phase power electronic devices in low voltage side has increased harmonic pollution in the power system to the larger extent. Improving power quality has become the biggest challenge for electrical engineers. A single phase shunt active power filter was modeled in MATLAB/SIMULINK using hysteresis current controller and triangular current controller. Simulation results are presented to demonstrate performance of single phase shunt active power filter during presence of nonlinear load. An experimental setup is established to validate the simulation result.

TABLE OF CONTENTS

CERTIFICATE	i
ACKNOWLEDGEMENT	iii
ABSTRACT	iv
TABLE OF CONTENTS	v
LIST OF FIGURES	viii
ABBREVIATIONS AND ACRONYMS	ix

CHAPTER-1

INTRODUCTION

1.1 BACKGROUND	2
1.2 MOTIVATION OF PROJECT WORK	3
1.3 OBJECTIVES OF PROJECT WORK	4

CHAPTER-2

HARMONICS AND HARMONIC COMPENSATION SCHEMES

2.1.SOURCES OF HARMONICS	7
2.2.HARMONIC REDUCTION AND REACTIVE POWER	7
2.3.COMPENSATION TECHNIQUES	7
2.3.1. PASSIVE FILTER	7
2.3.2. ACTIVE POWER FILTER	9

CHAPTER-3

LITERATURE REVIEW OF SHUNT ACTIVE POWER FILTER

3.1 SHUNT ACTIVE POWER FILTER	11
3.2 SYNCHRONOUS DETECTION METHOD	11
3.3 SYNCHRONOUS REFERENCE FRAME ALGORITHM	12

3.4 PEAK DETECTION METHOD	13
---------------------------	----

CHAPTER-4

MODELING AND SIMULATION

4.1 MATHEMATICAL MODELLING	15
4.2 SINGLE PHASE SHUNT ACTIVE POWER FILTER	16
4.3 DESIGN OF CONTROLLER	16
4.3.1 OUTER DC LINK VOLTAGE CONTROLLER	17
4.3.2 HYSTERESIS CURRENT CONTROLLER	17
4.3.3 TRIANGULAR CARRIER CURRENT CONTROLLER	19
4.4 SIMULATION RESULTS	20

CHAPTER-5

EXPERIMENTAL SETUP DESCRIPTION

5.1 INTRODUCTION	31
5.2 EXPERIMENTAL SETUP	31
5.2.1 SINGLE PHASE VARIAC	32
5.2.2 IGBT BASED INVERTER	32
5.2.3 SINGLE PHASE RECTIFIER	33
5.2.4 SIGNAL CONDITIONING CIRCUIT	33
5.2.4.1 CURRENT SENSOR	34
5.2.4.2 VOLTAGE SENSOR	36
5.2.4.3 GATE DRIVER	39
5.2.4.4 FILTER INDUCTOR	40

CHAPTER-6

CONCLUSION

6.1 CONCLUSION	42
----------------	----

REFERENCES	43
APPENDIX-A	44
APPENDIX-B	45
APPENDIX-C	46
APPENDIX-D	47

LIST OF FIGURES

1.1: Block diagram for active power filter connected system	12
2.1 Block diagram for passive filter connected power system	16
4.1: Control algorithm for generation of reference current and gate pulse	21
4.2 Power circuit diagram of single phase APF connected system	22
4.3: DC link PI controller	23
4.4: Hysteresis logic	24
4.5: Hysteresis Controller implemented in MATLAB SIMULINK	25
4.6: Triangular Carrier Controller implemented in MATLAB SIMULINK	26
4.7: Source voltage	27
4.8: Zoomed version of source voltage	27
4.9: Source current & load current	27
4.10: Zoomed version of source current & load current	27
4.11: Filter current	28
4.12: Zoomed version of filter current	28
4.13: Tracking of DC link voltage	28
4.14: Zoomed version of tracking of DC link voltage	28
4.15: Phase relationship between source voltage and source current	29
4.16: Zoomed version of phase relationship between source voltage and source current	29
4.17: Reactive power compensation	29
4.18: Gate pulses waveform	30
4.19: Zoomed version of gate pulse waveform	30
4.20: THD of source current before use of active power filter	30
4.21: THD of source current after use of active power filter	31
4.22: Source voltage	31
4.23: Zoomed version of source voltage	31
4.24: Source current & load current	32
4.25: Zoomed version of source current & load current	32
4.26: Filter current	32
4.27: Zoomed version of filter current	33
4.28: Tracking of DC link voltage	33
4.29: Phase relationship between source voltage and source current	33
4.30: Zoomed version of phase relationship between source voltage and source current	34

4.31: Reactive power compensation	34
4.32: Zoomed version of gate pulse waveform	34
4.33: THD of source current before use of active power filter	35
4.34: THD of source current after use of active power filter	35
5.1: Entire experimental set up	36
5.2: Single phase variac	36
5.3: DC link capacitor	36
5.4: IGBT based VSI	37
5.6: Working principle of current sensor	39
5.7: Schematics of current sensor	39
5.8: Current sensor card	39
5.9: Linear relationship between sensor output voltage and input current	41
5.10: Voltage sensor card	42
5.11: Working principle of voltage sensor	42
5.12: Linear relationship between sensor output voltage and input current	43
5.13: Gate driver output	44
5.14: Schematics of gate driver circuit	45
5.15: Gate driver card	45

ABBREVIATIONS AND ACRONYMS

SCR	-	Silicon Controlled Rectifier
IGBT	-	Insulated Gate Bipolar Transistor
MOSFET	-	Metal Oxide Semiconductor Field Effect Transistor
APF	-	Active Power Filter
PCC	-	Point of Common Coupling
SMPS	-	Switched Mode Power Supply
AC	-	Alternating Current
DC	-	Direct Current
PI	-	Proportional Integral
THD	-	Total Harmonic Distortion
PWM	-	Pulse Width Modulation
VSI	-	Voltage Source Inverter
SAPF	-	Shunt Active Power Filter
HVDC	-	High Voltage Direct Current

CHAPTER 1

Introduction

1.1 Background

Power quality improvement has become a major research topic in modern power distribution system. Nearly twenty years ago most of the loads used by the industries and consumers were passive and linear in nature, with a lesser number of non-linear loads thus having less impact on the power system. With the arrival of semiconductor and power electronic devices and their easier controllability have caused wide use of non-linear loads such as chopper, inverter switched mode power supply, rectifier, etc. The power handled by modern power electronics devices like silicon controlled rectifier (SCR), Insulated gate bipolar transistor (IGBT), power diode, Metal oxide semiconductor field effect transistor (MOSFET) are very large, which promotes their industrial as well as domestic applications. With addition to that various power electronic devices are used to increase the efficiencies and power factor of wind, solar, and other non-conventional sources of energy. While the advantages of using above devices are certainly good but there are some demerits of such excessive use of power electronic devices. The use of above semiconductor devices is responsible for harmonic and reactive power disturbances. The harmonics and reactive power are the cause various problem which includes overheating of transformers, excessive neutral current, distortion of feeder voltage, low power factor, damages to power electronic devices and malfunction of sensitive equipment [1]. To eliminate the harmonics in the power system, active power filters (APF) are installed at PCC. APF injects compensating current at PCC to cancel out the harmonics and to make source current sinusoidal. By installation of APF, harmonic pollution as well as low power factor in the power system can be improved. Though APFs are widely used in three phase system, by little modification in the control strategy it can be implemented in the single phase system, thus harmonic pollution can be reduced at low voltage system.

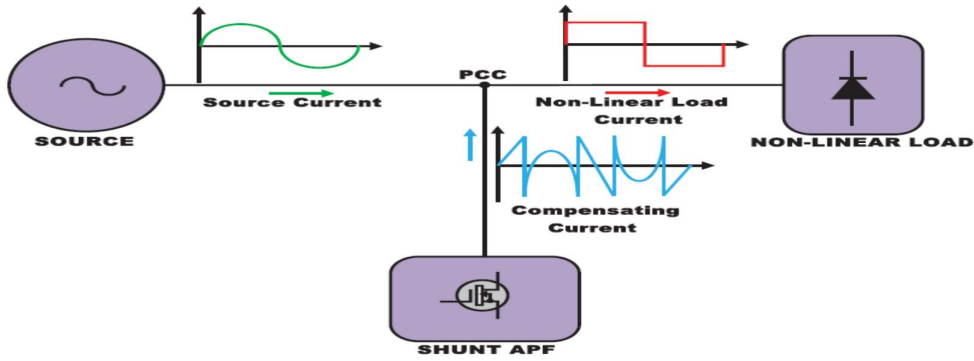


Fig.1 Block diagram for active power filter connected system

1.2 Motivation of Project Work

Harmonic pollution in low voltage side is more prominent compare to high voltage side due wide use of nonlinear single phase loads (Computers, Battery charger, Printers etc.), which is unacceptable. It is a huge challenge to nullify the undesirable current harmonics and compensate the reactive power requirement in the power system. The performances of traditional practices (use of LC filter) are not acceptable due to its serious drawbacks as discussed. The shunt APF provides encouraging results compare to traditional one based up on appropriate control algorithms. The control strategy play a key role for better dynamic performances of the APF. Most of the existing control schemes used for active power filter involve three phase quantity. By little modification, those control strategies can be used for single phase system. The synchronous detection method is used for three phase active power filter; this project work proves that synchronous detection method can be used for single phase active power filter which involves lesser complexities compare to that of instantaneous reactive power algorithm.

1.3 Objectives of Project Work

The objectives of this project are

- To discuss effect of harmonics arising due to nonlinear load
- To study different control strategies already proposed for modeling of 3 phase shunt active power filter
- To model and simulate single phase active power filter in MATLAB/SIMULINK environment
- Design of hysteresis current controller
- Design of triangular carrier current controller
- Experimental validation of simulation work

1.4 Organization of Thesis

The thesis is divided into 6 chapters including the chapter introduction. Each chapter is different from each other and is described with necessary theory and diagrams to understand it.

Chapter 2 deals with harmonics, causes of harmonics and the effect of harmonics on power system. Various schemes used to compensate harmonic is also discussed in this chapter. Previously passive filter was used to eliminate harmonics but due to their poor dynamic performances they are replaced by active power filter. The modern trend of eliminating harmonic is to use active power filter.

Chapter 3 presents literature review of shunt active power filter and its control strategy. Shunt active power filter nullify the effect of harmonics by injecting complementary component of harmonics being generated by nonlinear loads. The dynamic performances of shunt active power filter depend upon the control strategy adopted to generate the reference current. In this chapter various control algorithms like synchronous detection method, synchronous reference frame algorithm and peak detection method are discussed.

Chapter 4 presents mathematical modeling and simulation of single phase shunt active power filter. From the knowledge of load voltage and load current, power consumed by nonlinear load is calculated. By knowing load power, reference source current is generated. This reference current is compared with actual source current and the error signal is processed through a current controller to generate gate pulses for VSI. This chapter also deals with design of controllers like hysteresis current controller and triangular current carrier controller. Various simulation results are given for both the controller to observe their performances.

Chapter 5 deals with description of various hardware components required to establish experimental setup for single phase shunt active power. It also deals with calibration of current sensor and voltage sensor.

Chapter 6 gives comparative analysis of the simulation results between hysteresis controller based active power filter and triangular carrier controller based active power filter.

CHAPTER 2

Harmonics and Harmonic Compensation Schemes

2.1 Source of Harmonics

The term ‘Harmonic’ refers to a component with a frequency that is an integral multiple of the fundamental frequency. Harmonics in power system arises due to wide use of nonlinear loads. The major causes of current and voltage harmonics are due to energy conversion techniques and control involved in the power electronic devices such as rectifier, chopper, cyclo-converter etc. Energy conversion devices like voltage controller devices of motor, HVDC power converters, battery-charging systems, power factor improvement devices, traction, static-var compensators, direct energy devices-fuel cells, wind and solar-powered dc/ac converters, storage batteries which require dc/ac power converters, control of heating elements cause harmonic pollution in power system [7].

2.2 Harmonic Reduction and Reactive Power Compensation Techniques

The harmonic filter connected to AC system has two objectives

1. To minimize the effect of harmonic voltage and current in the power system below an acceptable level.
2. To compensate the reactive power required by the loads.

Two type of filters used for the above purposes which are

- Passive filter
- Active power filter

2.2.1 Passive Filter

The passive filter requires resistors, inductors, and capacitors and they do not depend upon any type of external power source. By proper selection of L and C , they are tuned to bypass a particular harmonic component. Multiple numbers of passive filters are connected in parallel to nullify higher order of harmonics as shown in Fig.1. Though passive filters were widely used as harmonic improvement and reactive power compensation devices in the power distribution system, their performances is not satisfactory due to following reasons:

- A separate filter is necessary for each harmonic frequency.
- Passive filter must be designed in considering with current provided by nonlinear load.
- Source impedance affects the compensation characteristics of *LC* filters.
- When the content of harmonics in the AC line increases, the filter will be loaded.
- Frequency variation of AC source and tolerances in the filter components will affect the compensation characteristics of *LC* filters. If the system frequency varies in wide range, components required for attaining tuned frequency become impracticable.

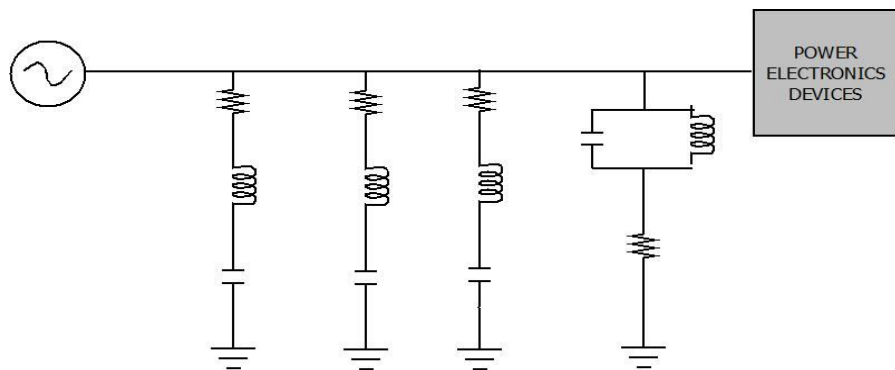


Fig.2 Block diagram for passive filter connected power system

With the above mentioned disadvantages the passive filter are less frequently used compared to active power filter. The practice of using the active power filter is the future trend of harmonic improvement in power distribution system because of its excellent dynamic characteristics. A flexible and handy solution to harmonic problem is provided by active power filters. Presently they are based on PWM converters and connected to low and medium voltage distribution system either in shunt or series.

2.2.2 Active Power Filter

Between different technical option available to eliminate harmonics and compensate reactive power in the power system, active power filter [11] system has been proved to be most prominent one. Active power filters (APF) are constructed using both passive and active elements. For their operation they need external power source. Presently available APFs are basically of pulse width modulated inverters (current source or voltage source). Current fed PWM inverter act as non-sinusoidal current source to cancel out the harmonic current produced by nonlinear load. Current fed PWM based APF's use is limited to low power application. Voltage source inverter (VSI) is the most popular one for implementing active power filtering. VSI based APFs have high power rating and lower switching frequency.

They are connected to AC mains through coupling reactors.

Active power filter can be classified into three categories as per their connection to the PCC, namely

1. Shunt active power filter
2. Series active power filter
3. Hybrid active power filter

But shunt active power filter is widely used due to its simpler construction and robustness. A brief idea about shunt active power filter and its control schemes are discussed in the next chapter.

CHAPTER 3

Literature Review of Shunt Active Power Filter

3.1 Shunt Active Power Filter

SAPFs are widely used in the power system to compensate reactive power and current harmonics. It can also play the role of static VAR generator in the power system for improving and stabilizing the voltage profile. Shunt active power filter compensate current harmonic by injecting complementary current that of produced by non-linear load. Shunt active power filter acts as a current source by introducing the harmonic components created by the load but phase shift by 180. Consequently, the current harmonic component present in the load current got cancelled and the source current remain sinusoidal and in phase with the respective phase to neutral voltage. By the use of proper control scheme, APF can also improve system power factor. Thus, by the effect of active power filter, voltage sources see the nonlinear load simply as resistor.

However the performances of SAPF largely depend on the control strategy which is responsible for generating complementary harmonic current to cancel out the current harmonics present in the load current. Various control strategies [2]-[6] for SAPF are discussed below

3.2 Synchronous Detection Method

Synchronous theory [4] can work efficiently under both balanced and unbalanced condition of source as well as load as the reference current are calculated considering the magnitude of each phase voltage separately. Current is distributed equally among three phases, to estimate the three phase compensating current to be provided by the active filter. Two assumptions are taken into consideration while calculating three phase reference currents i.e. Source voltage is not distorted and Peak magnitude of source currents are balanced after compensation as given in (1)

$$I_{rs} = I_{ys} = I_{bs} \quad (1)$$

Where I_{rs} , I_{ys} and I_{bs} are the amplitudes of three phase source current after compensating. The real power consumed by the load can be calculated as

$$P = \left[v_r v_y v_b \right] \cdot \begin{bmatrix} i_{Lr} \\ i_{Ly} \\ i_{Lb} \end{bmatrix} \quad (2)$$

Where, v_r , v_y and v_b are load voltages and i_{Lr} , i_{Ly} and i_{Lb} are load current. The active power P is sent through a low pass filter to obtain its average value P_{dc} . Then the active power is split into three phases as follows (3)

$$\left. \begin{array}{l} P_r = \frac{P_{dc} \cdot E_r}{E} \\ P_y = \frac{P_{dc} \cdot E_y}{E} \\ P_b = \frac{P_{dc} \cdot E_b}{E} \end{array} \right\} \quad (3)$$

Where E_r , E_y and E_b are the amplitudes of the source voltages e_r , e_y and e_b . E is the algebraic sum of E_r , E_y and E_b . The desired reference current can be calculated as (4)

$$\left. \begin{array}{l} I_{rl}^* = \frac{2 \cdot e_r \cdot P_r}{E_r^2} \\ I_{yl}^* = \frac{2 \cdot e_y \cdot P_y}{E_y^2} \\ I_{bl}^* = \frac{2 \cdot e_b \cdot P_b}{E_b^2} \end{array} \right\} \quad (4)$$

3.3 Synchronous Reference Frame Algorithm

This method is quite similar to instantaneous reactive power theory method. The important features of this algorithm [5] is that it require only load current for generating reference current and hence source disturbances or voltage distortion have no effect on the performances of active power filter system. As this method involves synchronous frame of

reference, a separate PLL is required for each phase to synchronize reference current with its corresponding phase to neutral voltage.

3.4 Peak Detection Method

In this method [5] distorted load current is filtered to extract fundamental component of load current. After obtaining fundamental component of load current, its phase is shifted by 180. If this current is added with distorted load current, it will give the waveform of current which is required to compensate only the harmonic distortion present in the load current. In order to compensate the reactive power required by the load, extracted fundamental component of load current has to be synchronized with its corresponding phase to neutral voltage.

CHAPTER 4

Modelling and Simulation

4.1 Mathematical Modeling

Fundamental component of current and voltage is responsible of delivering active power at the load end. This concept is used in synchronous detection method to generate reference current. Active Power consumed by load can be calculated as (5):

$$P = v_{load} \times i_{load} \quad (5)$$

This power can be decoupled as (6):

$$P = \bar{P} + \tilde{P} \quad (6)$$

\bar{P} (DC active power) is contributed by fundamental component of voltage and current while harmonic components are responsible for \tilde{P} (alternating active power). By filtering, the alternative part \tilde{P} can be removed and the reference current can be generated .The reference current is compared with the actual source current and the error signal is passed through controller (hysteresis or triangular carrier current controller) to generate gating pulses to drive voltage source inverter as shown in the block diagram in Fig.4.1

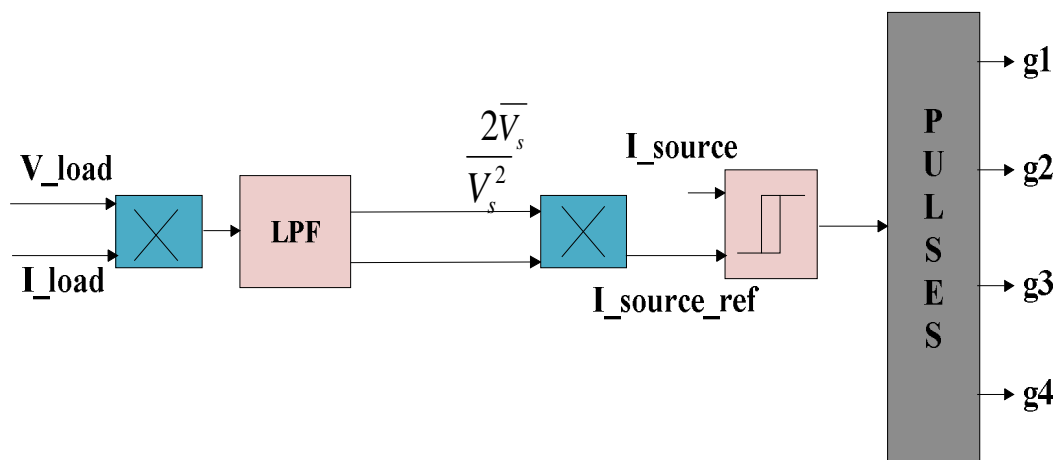


Fig.4.1 Control algorithm for generation of reference current and gate pulse

4.2 Single Phase Shunt Active Power Filter

Single phase shunt active filter consists of IGBT/MOSFET based inverter shunted with DC link capacitor. It is connected to point of common coupling through AC link reactor. The power circuit diagram of single phase shunt active power filter connected system is shown in the Fig.4.2 .It consists of single phase supply utility, single phase bridge rectifier, single phase IGBT based voltage source inverter, controller and load.

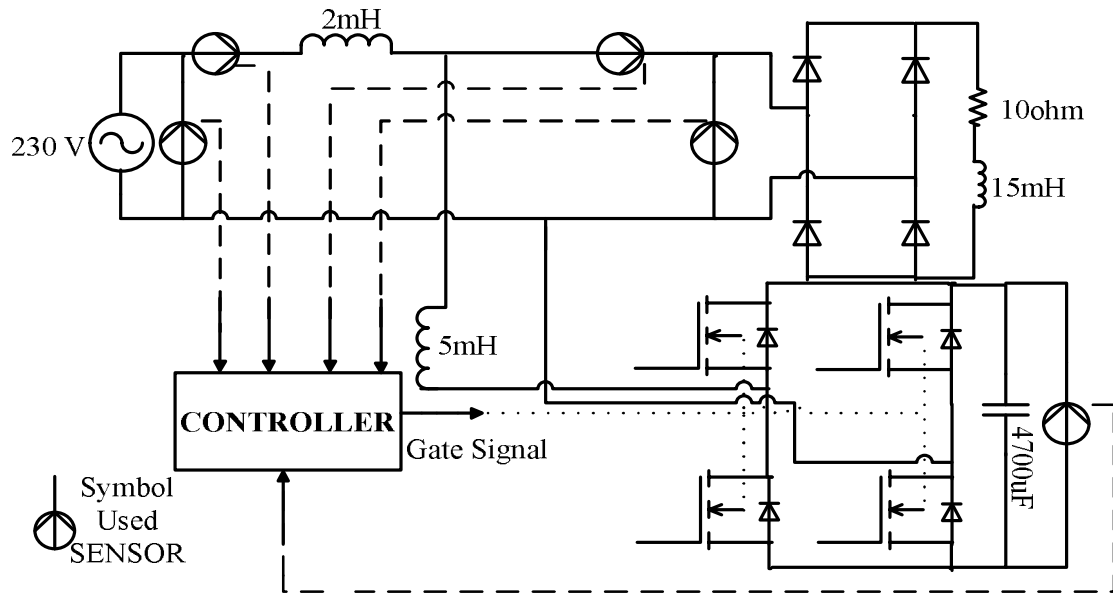


Fig.4.2 Power circuit diagram of single phase APF connected system

4.3 Design of Controller

The heart of the active power filter system is its controller. Proper control scheme enables active power filter to carry out harmonic elimination as well as reactive power compensation. The controller of shunt active power filter is divided into two parts i.e.

1. Inner current control loop
2. Outer DC link voltage control loop

4.3.1 Outer DC link Voltage Controller

To control DC bus voltage, it is required to take care of little amount of power flowing into DC capacitor, thus compensating for switching and conduction losses. The dc link voltage control loop does not require to be as fast as it respond to steady state operating condition. The actual DC link voltage is compared with a reference DC link voltage and passed through a PI controller. To maintain dc-link voltage at a fixed reference value, the dc-link capacitor requires a certain amount of real power, which is directly proportional to the difference between the reference and actual voltages. The control signal coming from PI controller to regulate DC link voltage can be expressed as

$$P_{dc_link} = K_p(v_{dc_ref} - v_{dc}) + K_i \int (v_{dc_ref} - v_{dc}) dt \quad (7)$$

Where, K_p and K_i are proportional and integral gains of the PI controller. By increasing proportional gain (K_p) reduces rise time and steady-state error but it causes increase in the overshoot and settling time. Similarly increase of integral gain (K_i) reduces steady state error but it increases overshoot and settling time. The block diagram is shown in the Fig 4.3

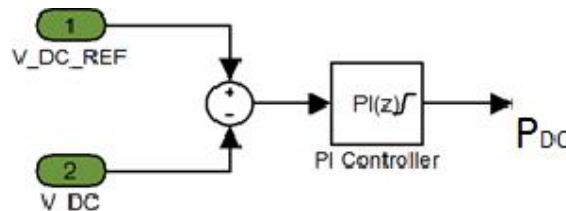


Fig.4.3 DC link PI controller

4.3.2 Hysteresis Current Controller

The hysteresis band current controller is used to generate pulses for the switching pattern of the inverter. There are numerous current control methods, but quick current controllability and easy implementation make hysteresis current control method much more superior than other current control methods. Some of the better properties possessed by hysteresis band current controllers are robustness, excellent dynamics and fastest control with minimum

hardware. This method switches the transistor when the current error fed to it exceeds the fixed band. Smaller the band width better is the accuracy. If current becomes more than the upper limit of the hysteresis band ($+h$), the switch in the upper part of the inverter arm becomes turned off and the switch in the lower arm becomes turned on. Hence, the current starts decreasing. While decreasing if the current falls below the lower limit of the hysteresis band ($-h$), the lower switch of the inverter arm becomes turned off and the upper switch becomes turned on. Consequently, the current gets back into the hysteresis band. So, the actual current is forced to follow the reference current within the hysteresis band. Operating principle of hysteresis current controller is depicted in the Fig.2.4 Variable switching frequency is the disadvantages of this method.

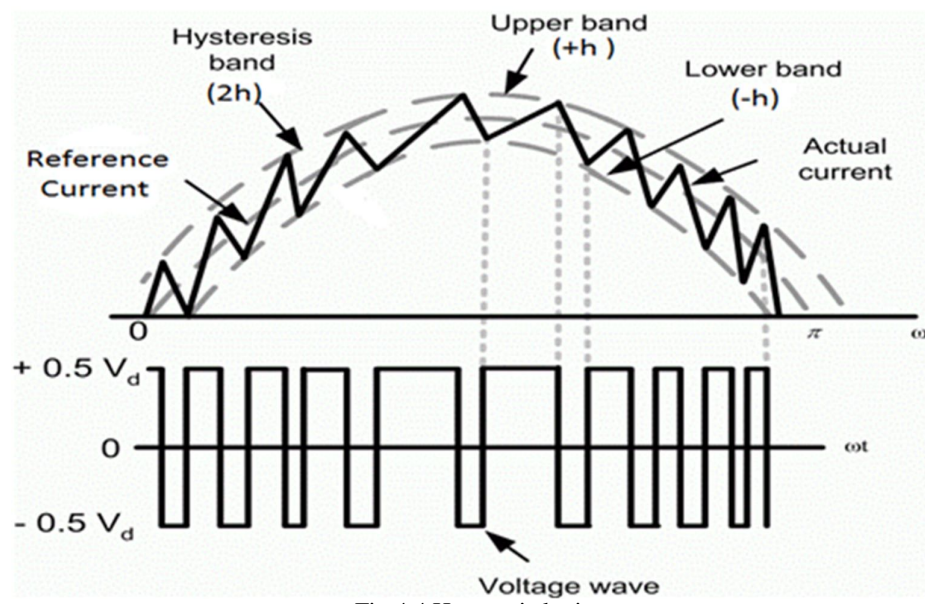


Fig.4.4 Hysteresis logic

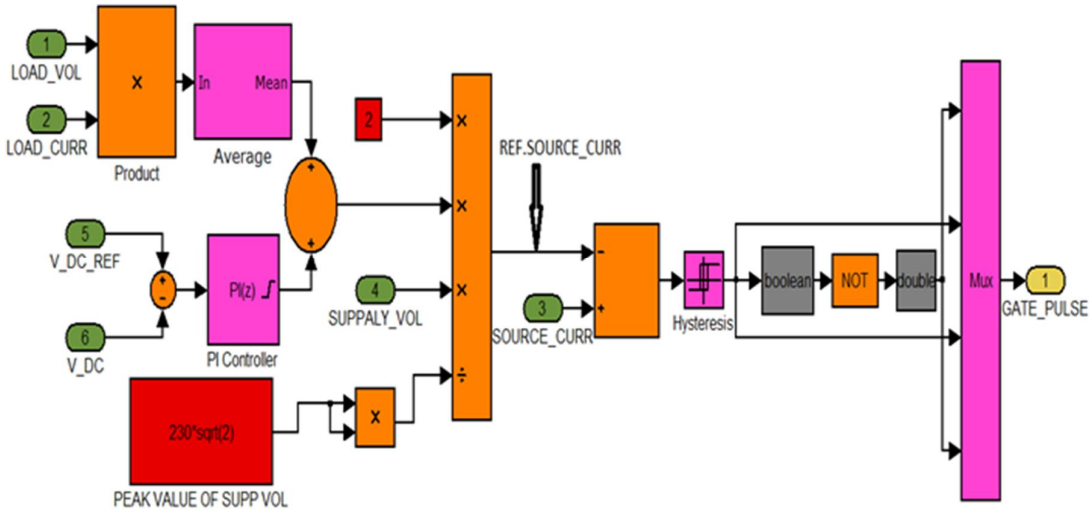


Fig.4.5 Hysteresis Controller implemented in MATLAB SIMULINK

4.3.2 Triangular Carrier Current Controller

In this method [5] the current error is compared with the fixed frequency and fixed amplitude of triangular carrier wave. The current error is passed through a proportional integral (PI) controller before comparison with the triangular carrier wave. When the carrier wave (Triangular wave) is smaller than the error signal, the gate signal is positive and upper switch will be turned on and lower switch will become turned off. When the carrier wave (Triangular wave) is larger than the error signal, the gate signal is zero, and upper switch will become turned off and lower switch will become turned on. This results in a gate pulse with variable width. Increasing proportional gain (K_p) decreases rise time and steady-state error but increases the overshoot and settling time. Increasing integral gain (K_i) reduces steady state error but increases overshoot and settling time. The frequency of the carrier wave determines the switching frequency. As switching frequency is known, switching losses can be predicted. Block diagram of triangular carrier current controller is depicted in the Fig.4.6.

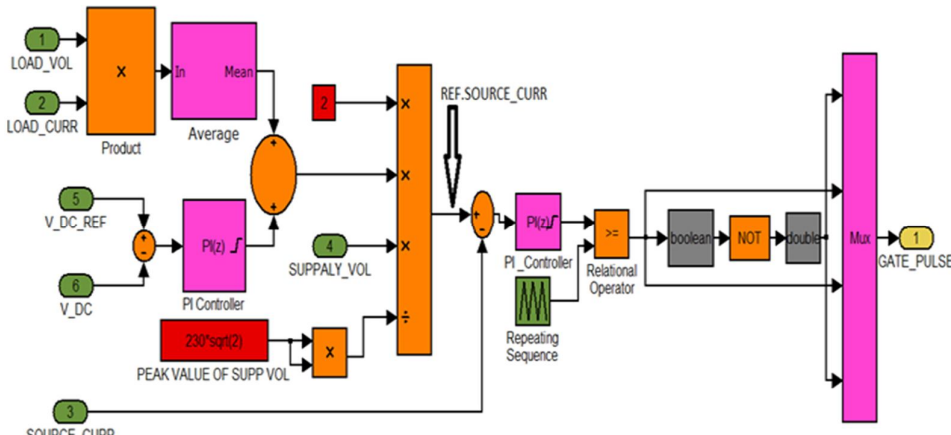


Fig 4.6 Triangular Carrier Controller implemented in MATLAB SIMULINK

4.4 Simulation Results

Single phase shunt active power filter system is simulated in MATLAB/SIMULINK environment. Various parameter used for simulation is given in the Table 4.1. The model was run for 0.2 second without connecting active power filter to PCC of power circuit and then active power filter was connected to the power circuit. At the time connecting active power filter to the power circuit, there is large increase in source current. This large current is known as inrush current which arises due to initially uncharged capacitor at the inverter end. It can be minimized by the use of thermistor in series with DC link capacitor.

Sl No.	Simulation Parameters	Ratings
1	Source Voltage	230V(r.m.s)
2	Source Inductance	1mH
3	Single Phase Bridge Rectifier	---
4	R-L Load	10 ohm, 50 mH
5	Filter Inductance	5 mH
6	IGBT/Diodes	---
7	DC Link Capacitor	4700 uF
8	DC Link Ref. Voltage	400V
9	Sampling Frequency (Ts)	1e-4
10	DC Link PI Controller	K _p =25, K _i =20
11	Hysteresis Current controller	Hysteresis Band=0.1
12	Triangular Carrier Current Controller	Switching Freq=1e+4 Sampling Frequency=1e+5

Table 4.1

4.5 Simulation Result for Hysteresis Current Controller Based APF

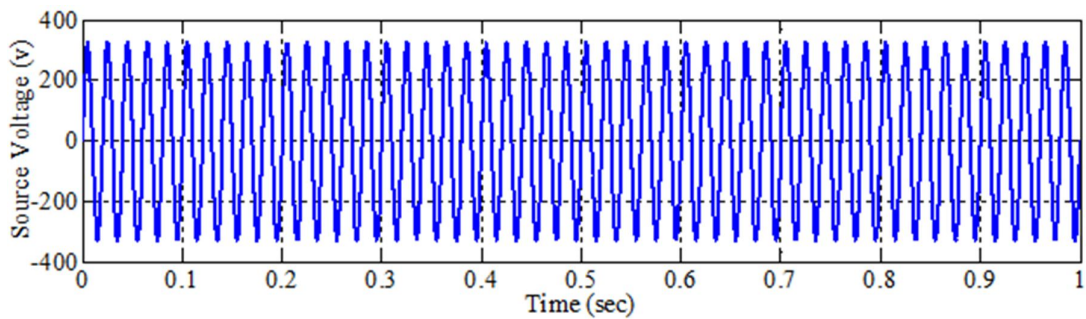


Fig.4.7 Source voltage

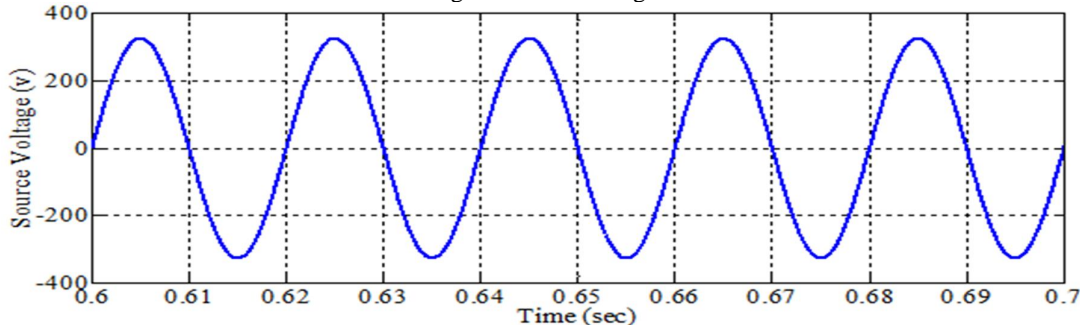


Fig.4.8 Zoomed version of source voltage (0.6 Sec to 0.7 Sec)

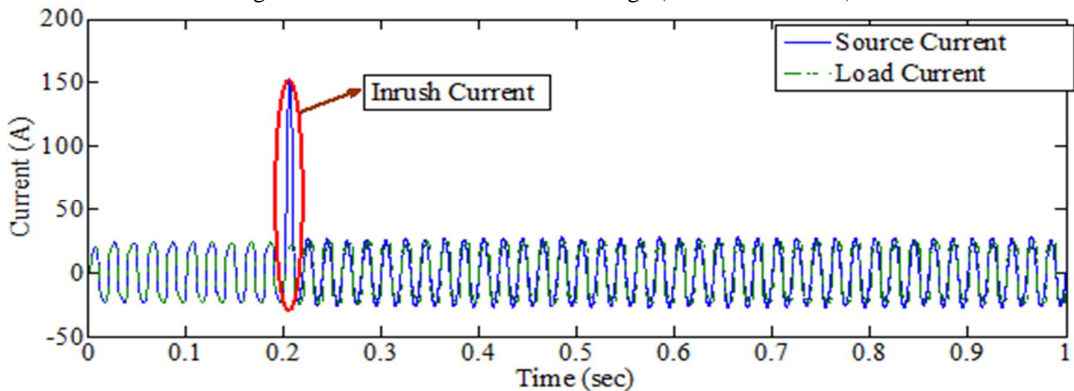


Fig.4.9 Source current & load current

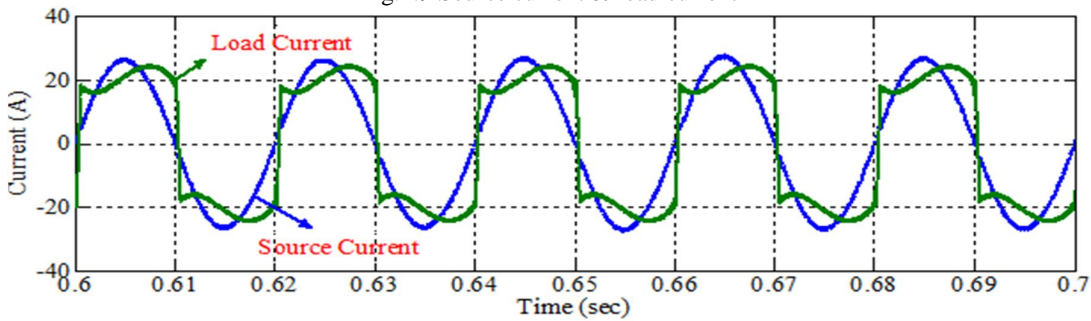


Fig.4.10 Zoomed version of source current & load current (0.6 Sec to 0.7 Sec)

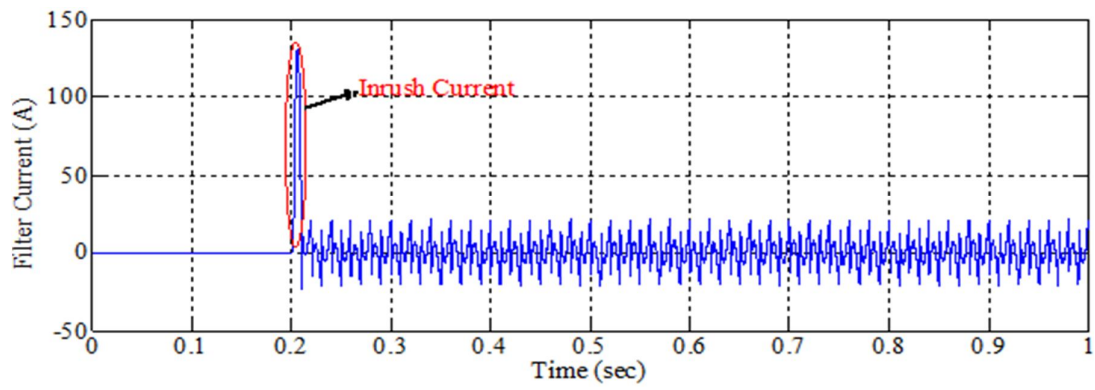


Fig.4.11 Filter current

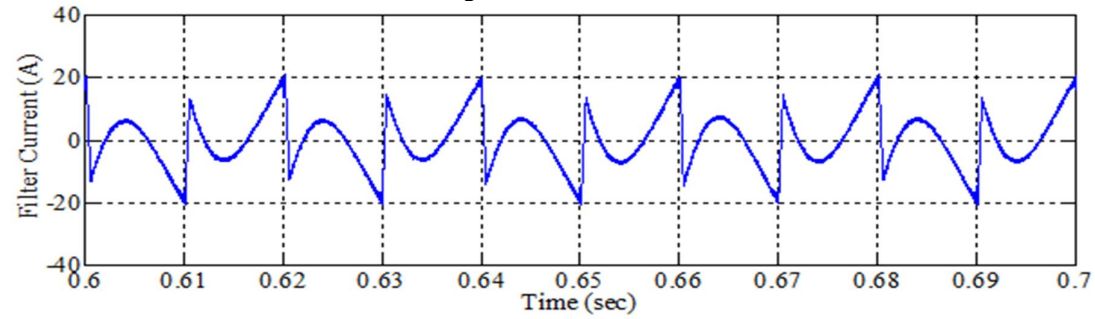


Fig.4.12 Zoomed version of filter current (0.6 Sec to 0.7 Sec)

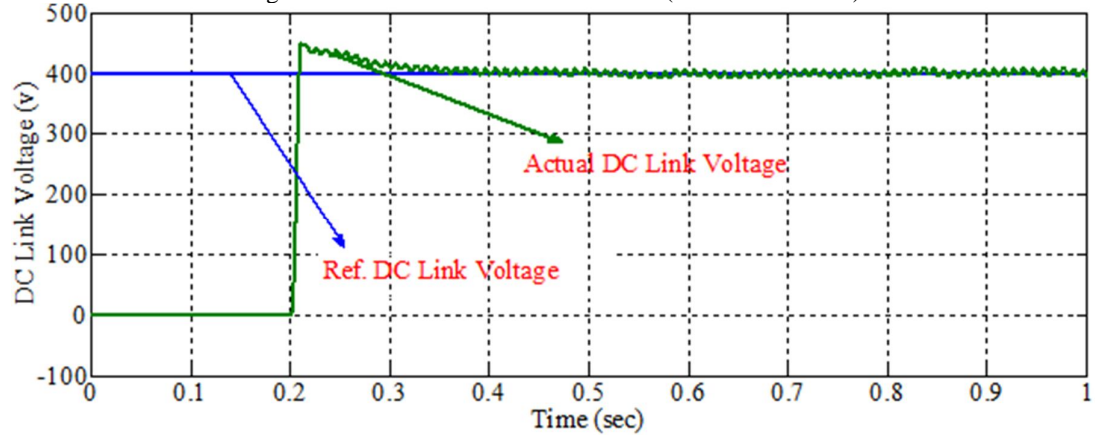


Fig.4.13 Tracking of DC link voltage

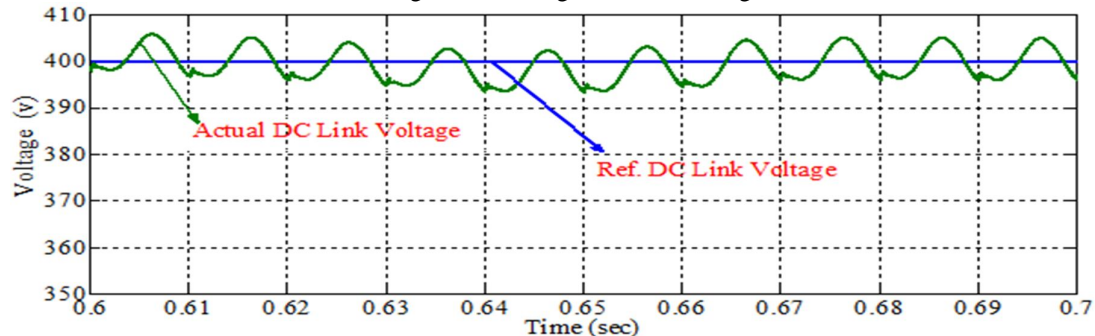


Fig.4.14 Zoomed version of tracking of DC link voltage (0.6 Sec to 0.7 Sec)

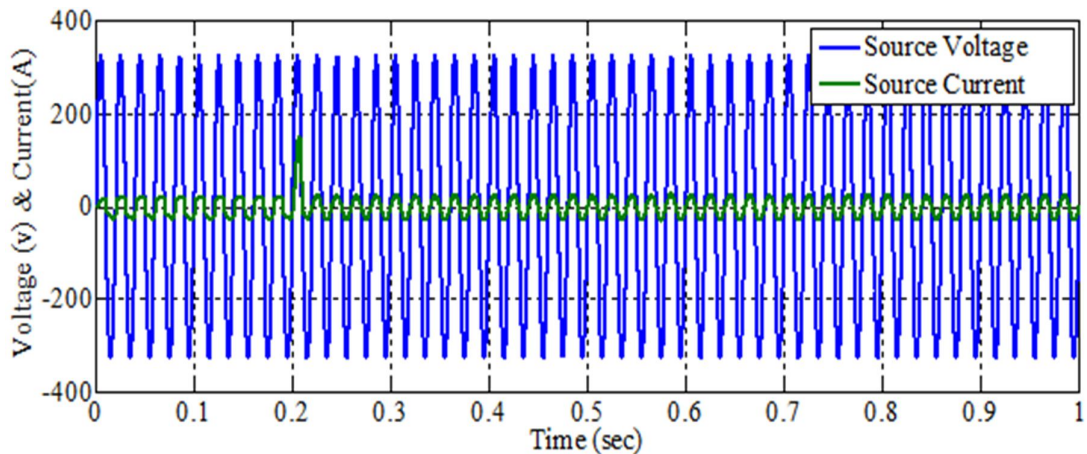


Fig.4.15 Phase relationship between source voltage and source current

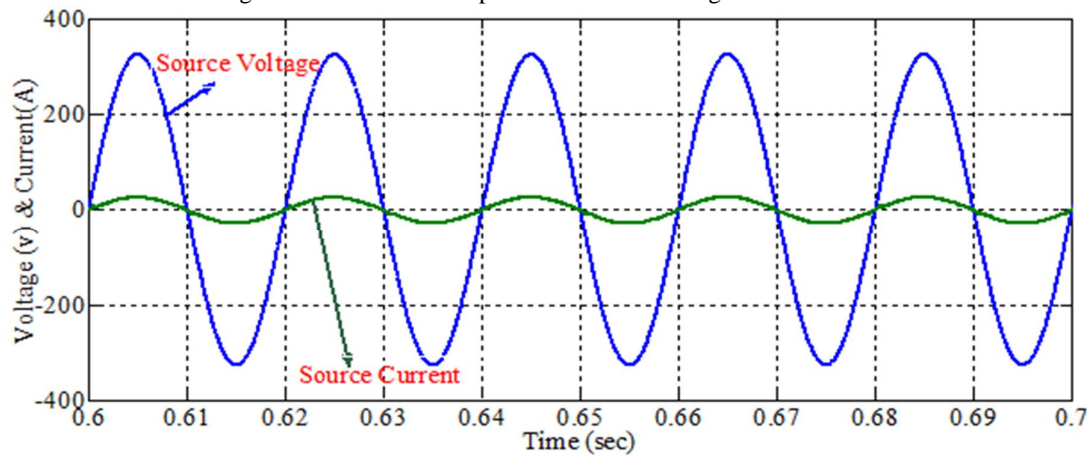


Fig.4.16 Zoomed version of phase relationship between source voltage and source current (0.6 sec to 0.7 sec)

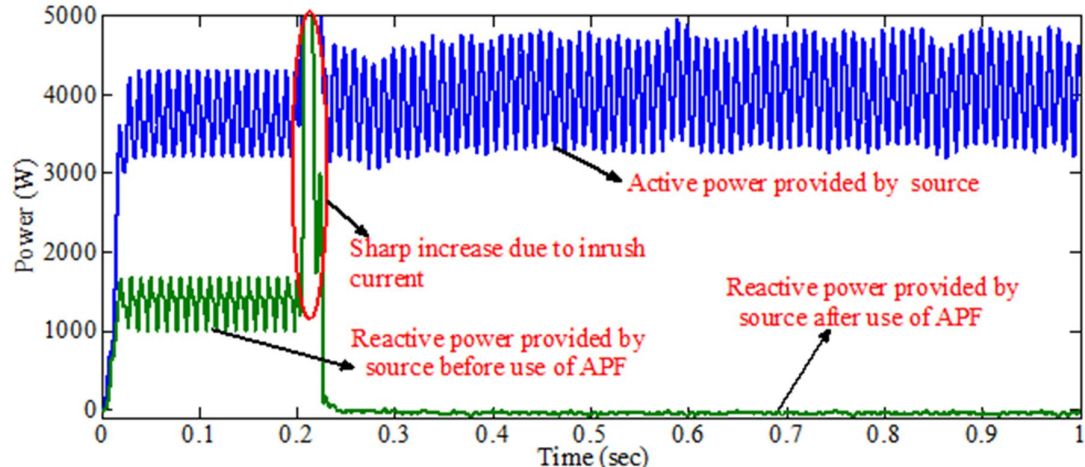


Fig.4.17 Reactive power compensation (Though y ordinate unit is in watt, for reactive power it will be treated as VAR)

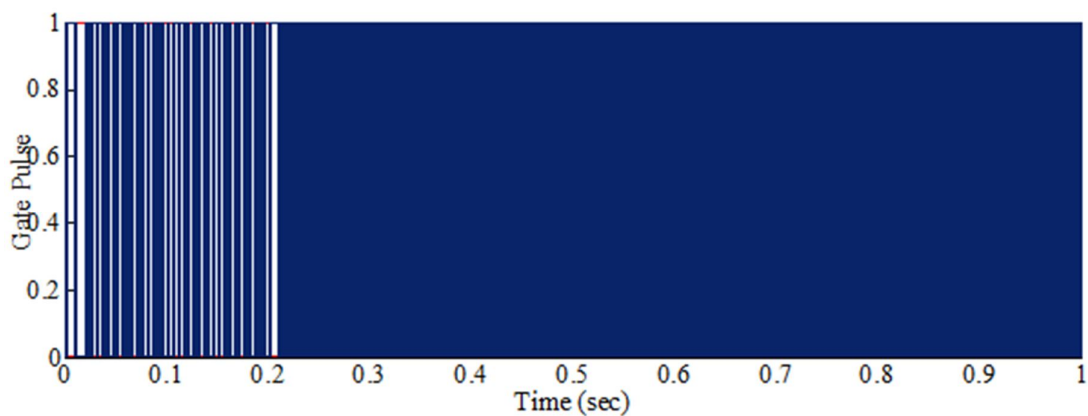


Fig.4.18 Gate pulses waveform

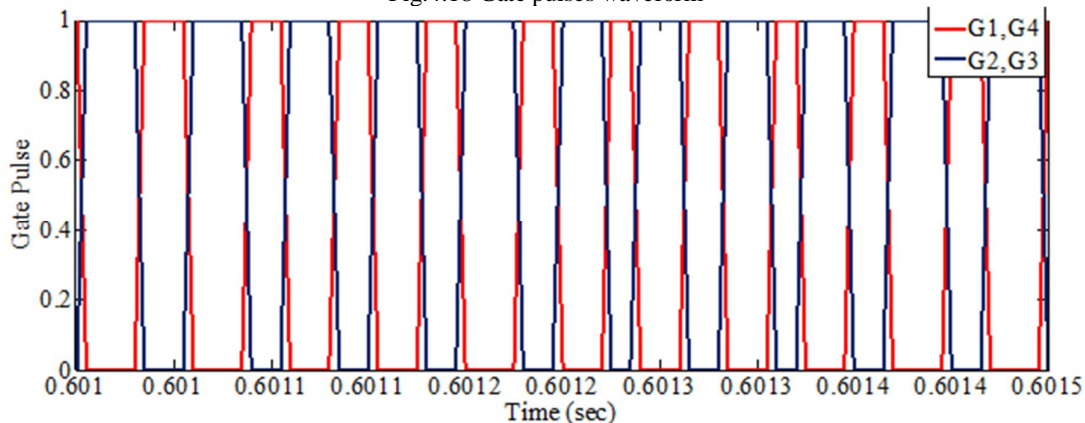


Fig.4.19 Zoomed version of gate pulses waveform (0.6 sec to 0.6015 sec)

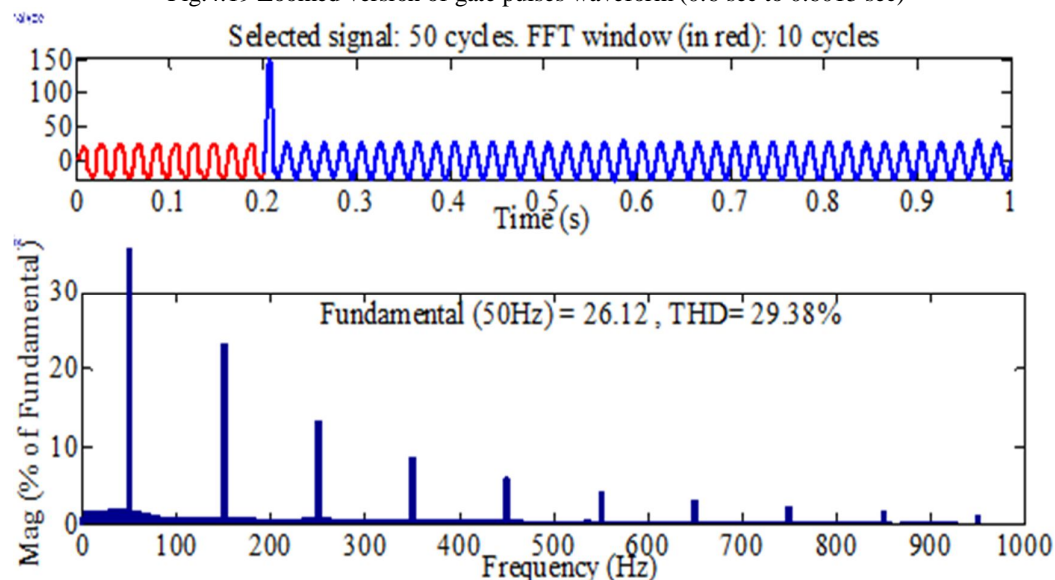


Fig.4.20 THD of source current before use of active power filter

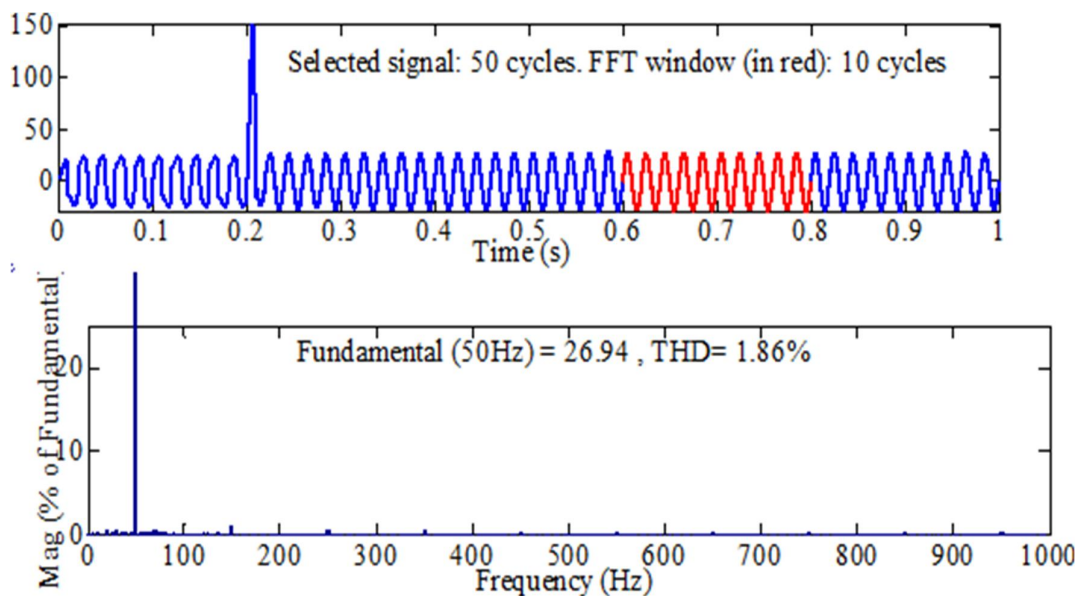


Fig.4.21 THD of source current before use of active power filter

4.6 Simulation Result for Triangular Carrier Current Controller Based APF

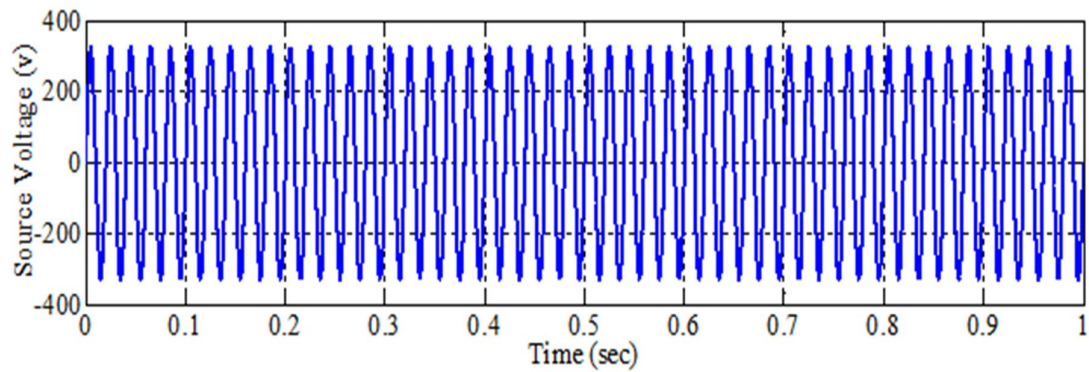


Fig.4.22 Source voltage

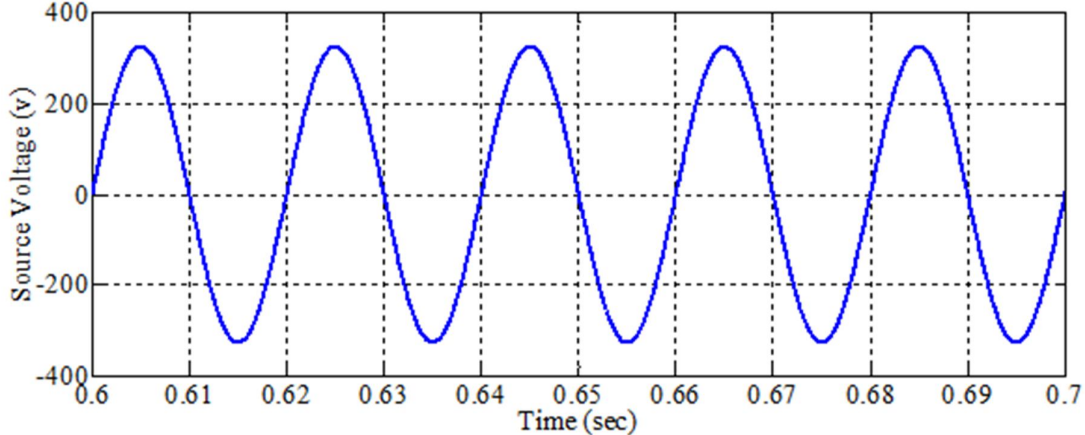


Fig.4.23 Zoomed version of source voltage (0.6 Sec to 0.7 Sec)

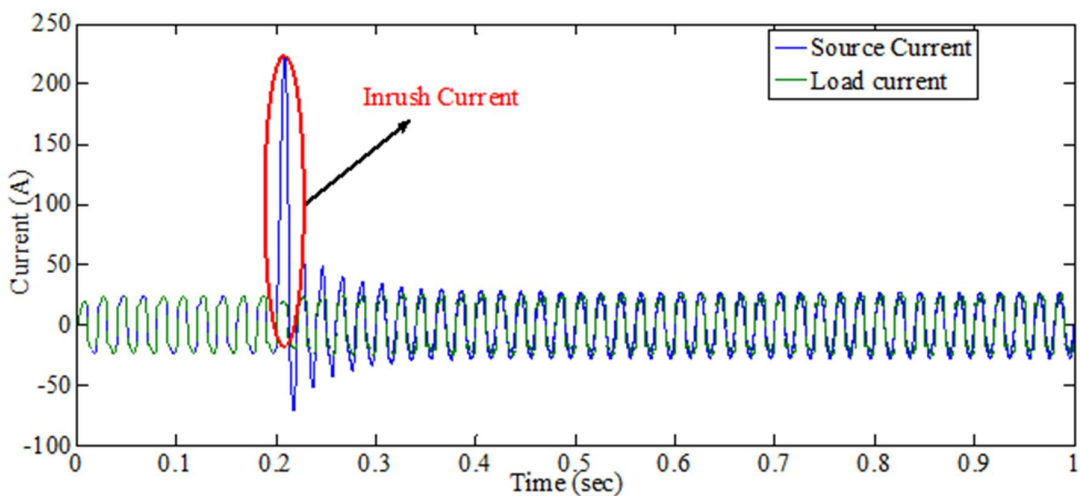


Fig.4.24 Source current & load current

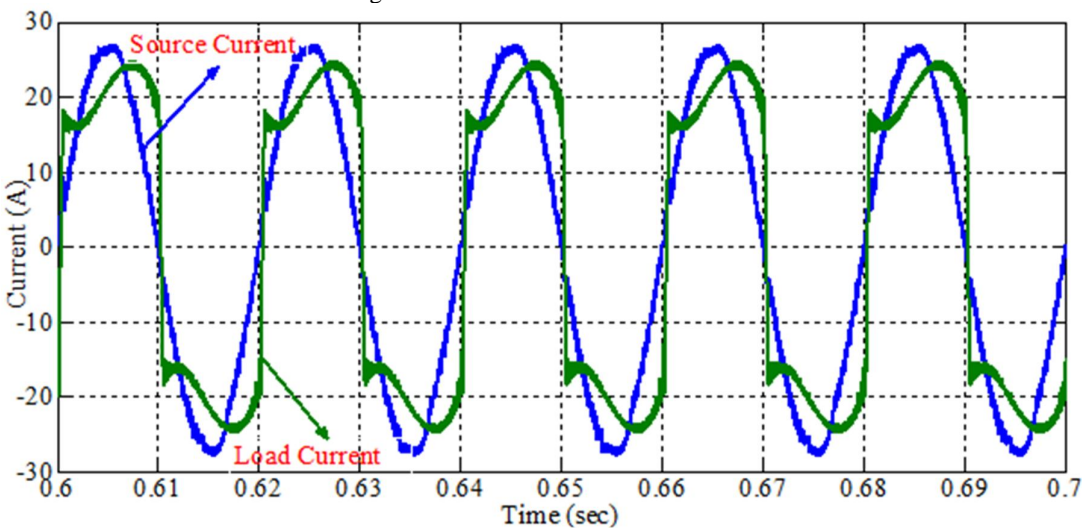


Fig.4.25 Zoomed version of source current & load current (0.6 Sec to 0.7 Sec)

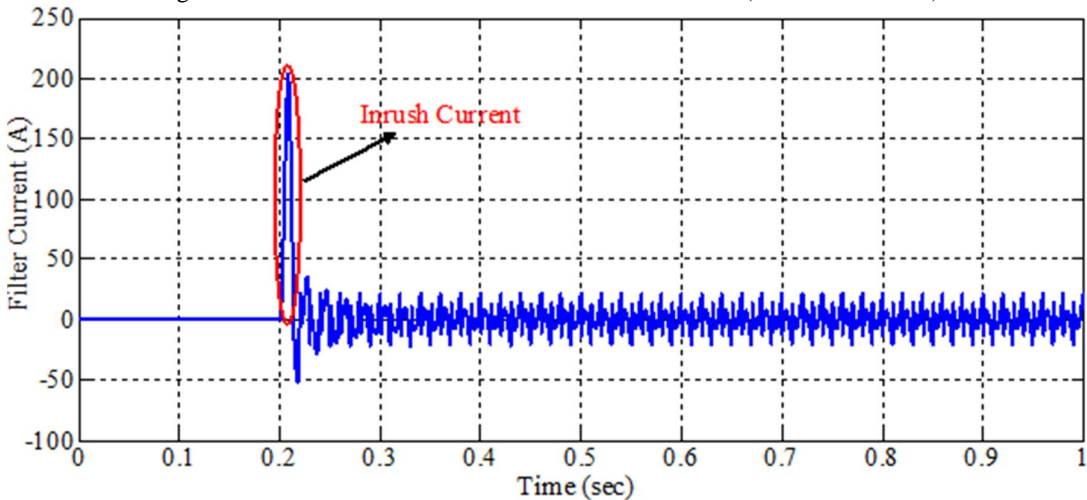


Fig.4.26 Filter current

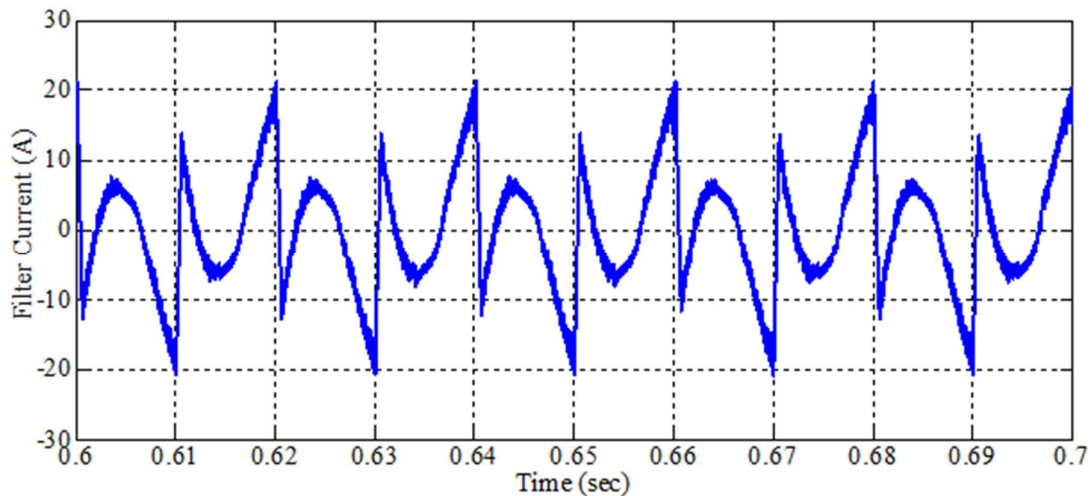


Fig.4.27 Zoomed version of filter current (0.6 Sec to 0.7 Sec)

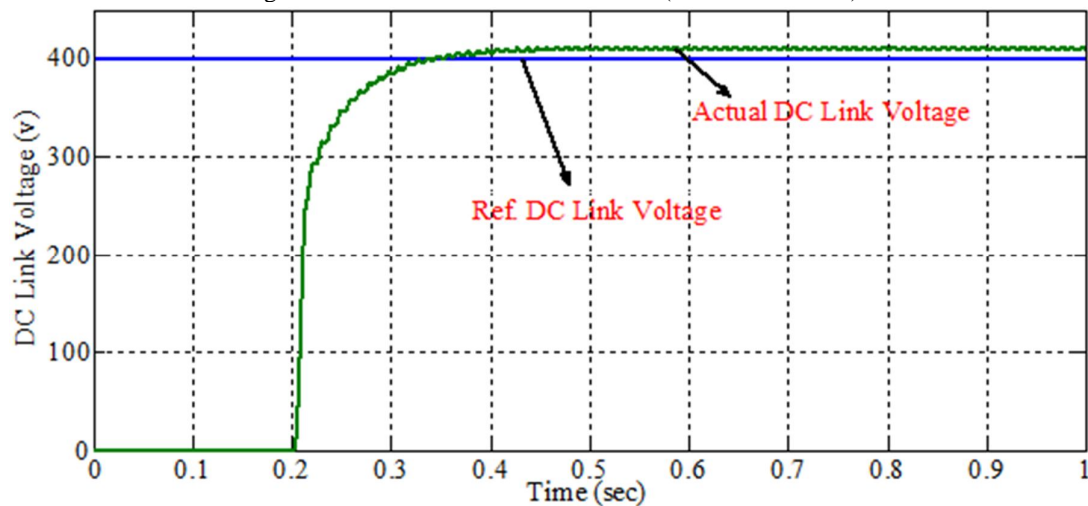


Fig.4.28 Tracking of DC link voltage

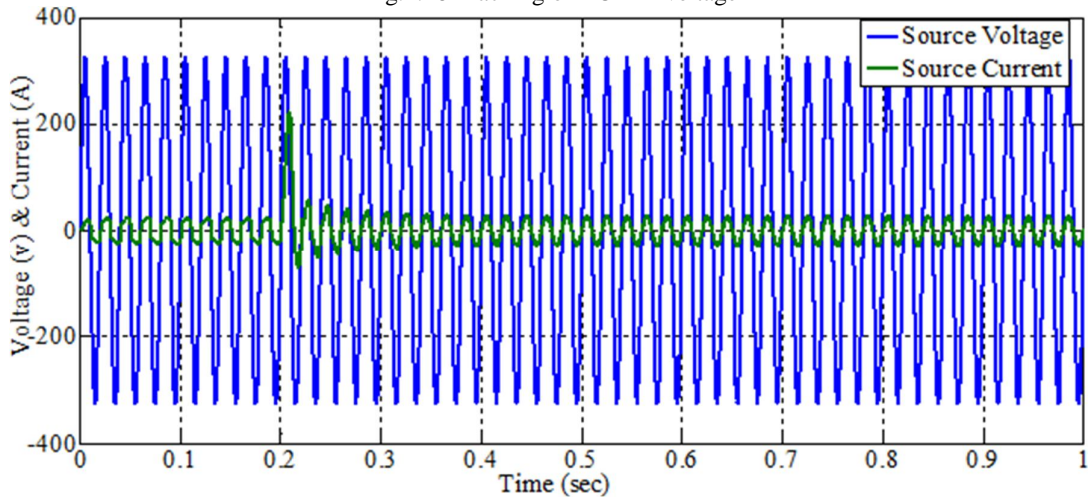


Fig.4.29 Phase relationship between source voltage and source current

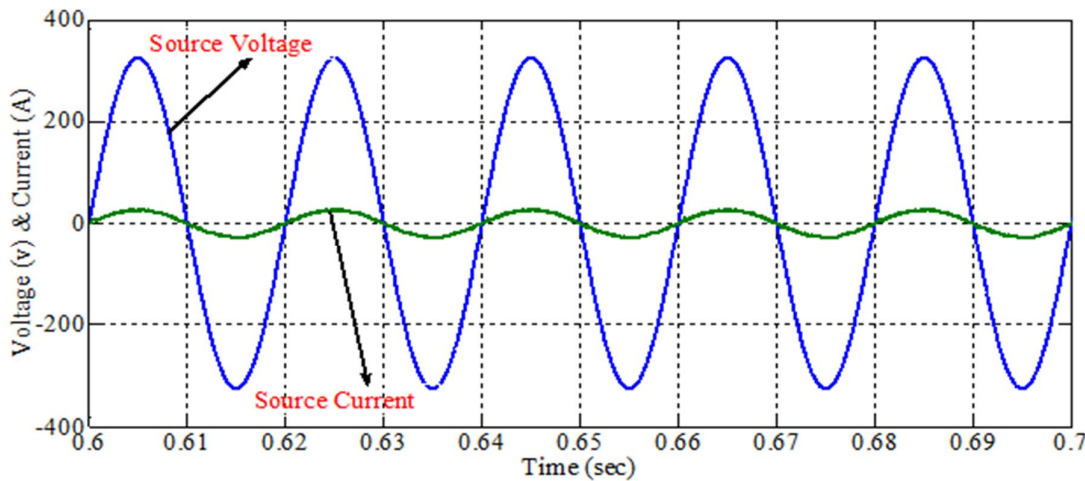


Fig.4.30 Zoomed version of phase relationship between source voltage and source current (0.6 sec to 0.7 sec)

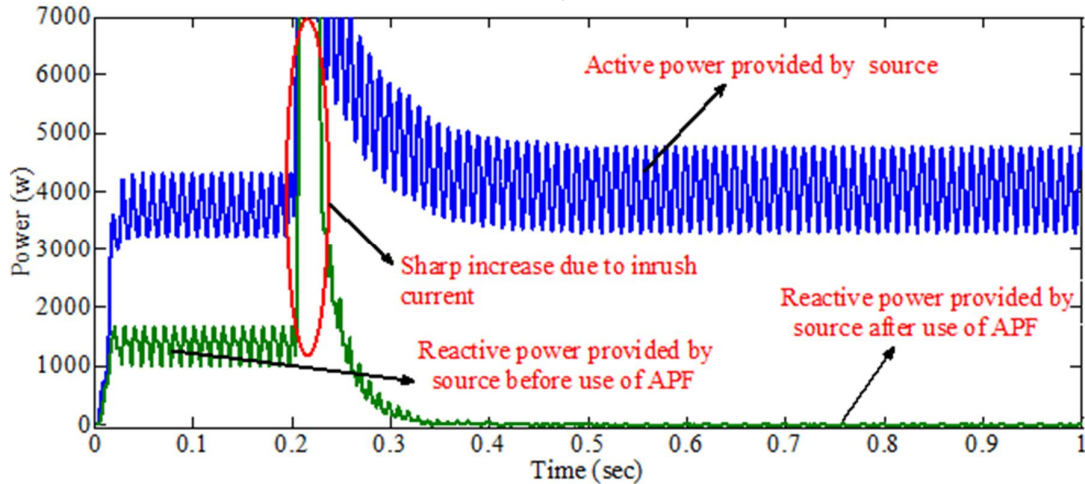


Fig.4.31 Reactive power compensation (Though y ordinate unit is in watt, for reactive power it will be treated as VAR)

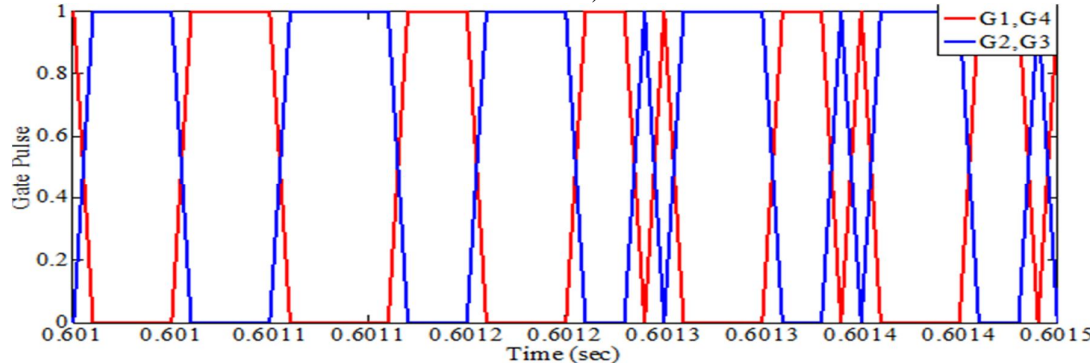


Fig.4.32 Zoomed version of gate pulses waveform (0.6 sec to 0.6015 sec)

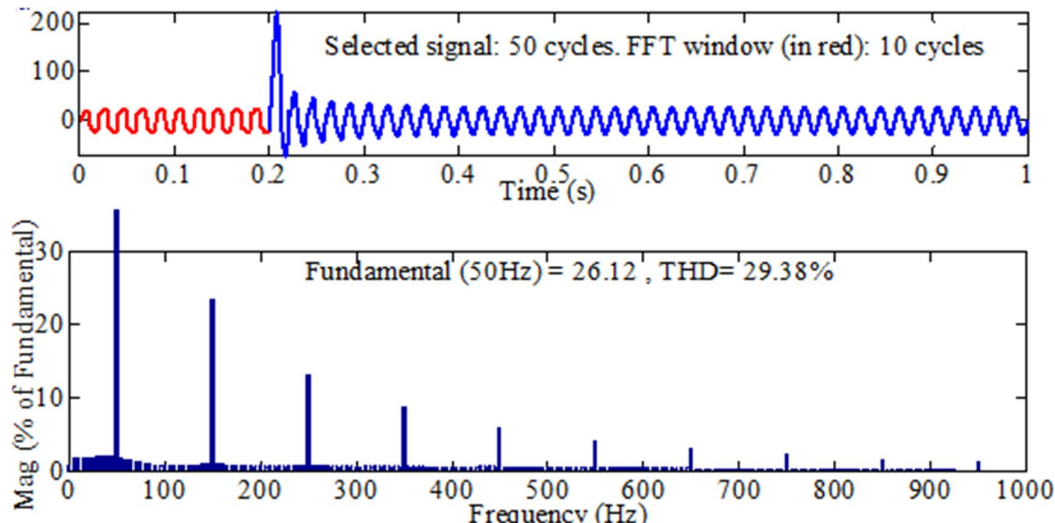


Fig.4.33 THD of source current before use of active power filter

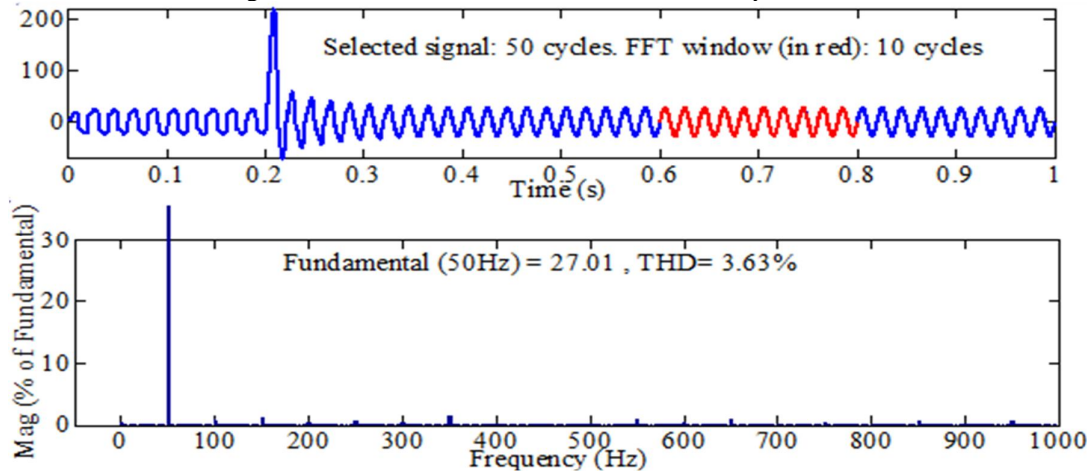


Fig.4.34 THD of source current before use of active power filter

CHAPTER 5

Experimental Setup Description

5.1 INTRODUCTION

A set up is developed to test the effectiveness of both circuit topology and control strategy.

Detail descriptions of individual hardware component, their circuit topology and output result are presented in this chapter.

5.2 EXPERIMENTAL SETUP

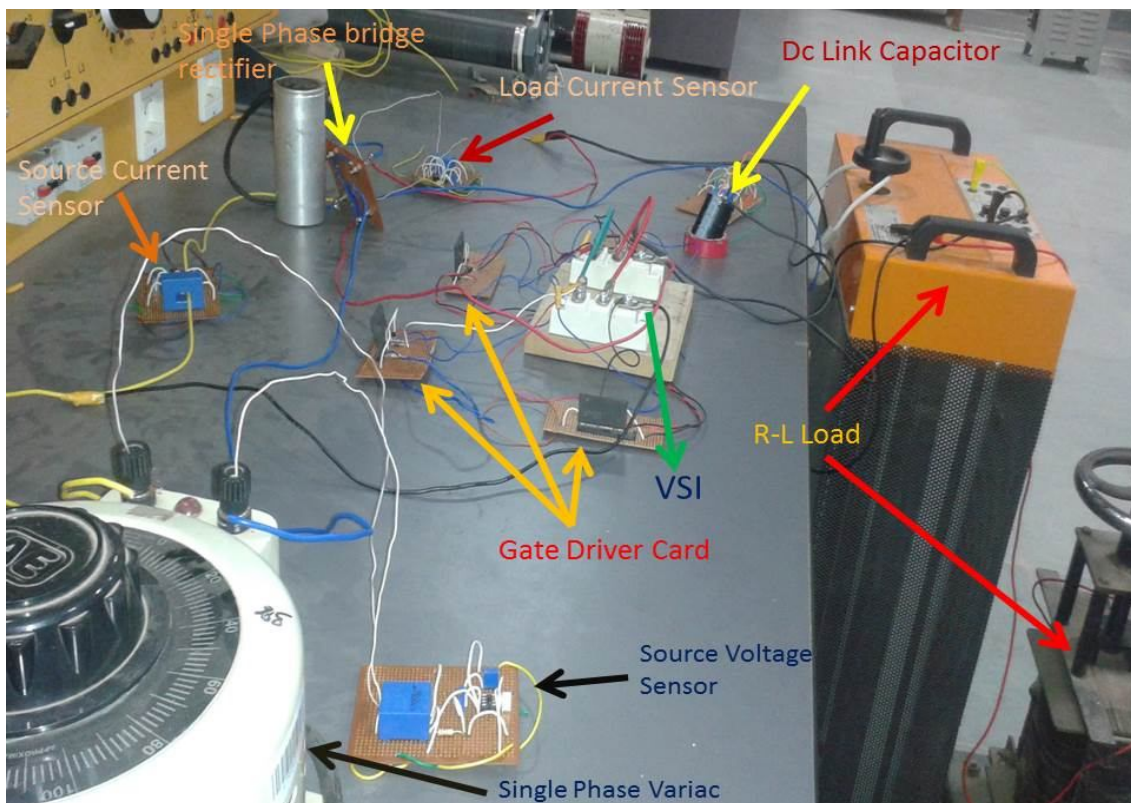


Fig.5.1 Entire experimental set up

The entire hardware set up used for experimental purposes can be categorized into

1. Single phase Variac
2. IGBT based inverter
3. Single phase rectifier
4. Signal conditioning circuit
5. Filter inductor

6. Source inductor
7. DC link capacitor
8. R-L load

5.1.1 Single Phase Variac

It is used as a sinusoidal voltage source to provide necessary supplied voltage required for experimental set up. For simplicity it is assumed that its output voltage waveform is pure sinusoidal.



Fig.5.2 Single phase variac

5.1.2 IGBT Based Inverter

Single phase voltage source inverter for the experiment is developed by using four IGBT's as the switching devices. The IGBT's used are of SEMIKRON, SKM150GB063D made (600 volt, 175 ampere) and will be driven by the gate driver card VLA517-01R. The DC link capacitor used in the inverter is of $470\mu\text{F}$ (500 volt, 25 ampere) and is shown in the Fig.5.3..The schematic of the developed VSI is shown in the Fig.5.4.



Fig.5.3 DC link capacitor

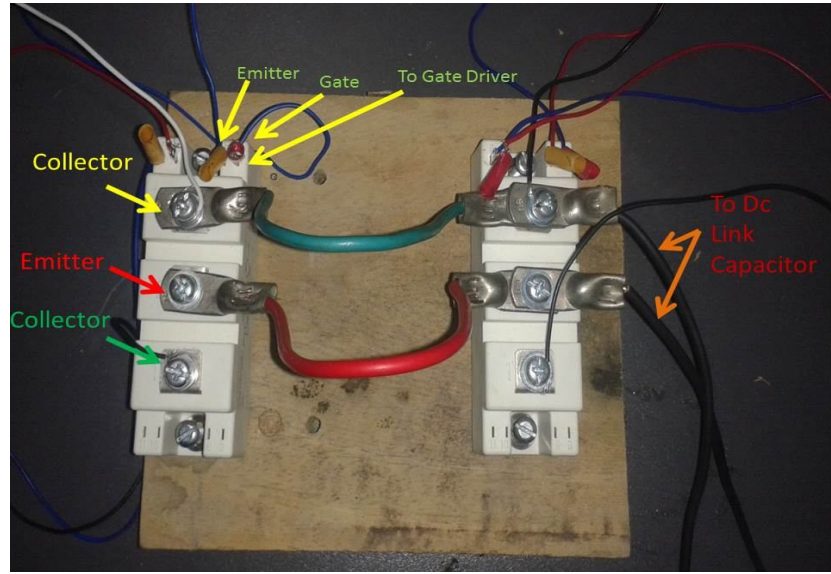


Fig.5.4 IGBT based VSI

5.1.3 Single Phase Rectifier

The combination of single phase rectifier and R-L load is used as a nonlinear load to create harmonics in the source current. The power diode used to construct Rectifier Bridge is of 15 ampere, 500 volt.

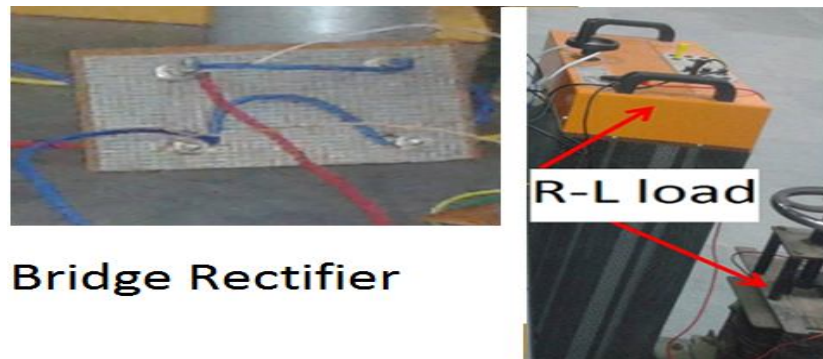


Fig.5.4 IGBT based VSI

5.1.4 Signal Conditioning Circuit

In this section the description of the different sensors and the gate driver card for the IGBT's of the VSI are described.

5.1.4.1 Current Sensor

For the control scheme, source current and load current have to be sensed. Two LEM manufactured current transducers LA 55-P, will be used to sense respective currents. The schematic of current sensor is shown in Fig.5.1.

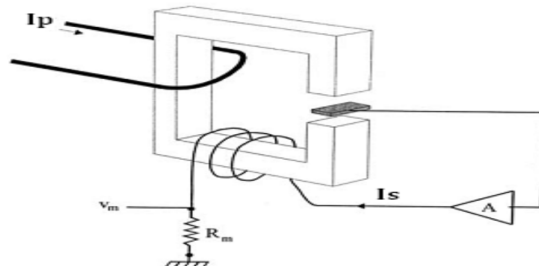


Fig.5.6 Working principle of current sensor

The magnetic flux created by the primary current is balanced through a secondary coil using a Hall device and associated electronic circuit.

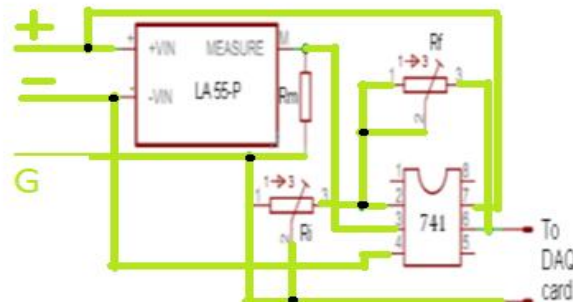


Fig.5.7 Schematics of current sensor

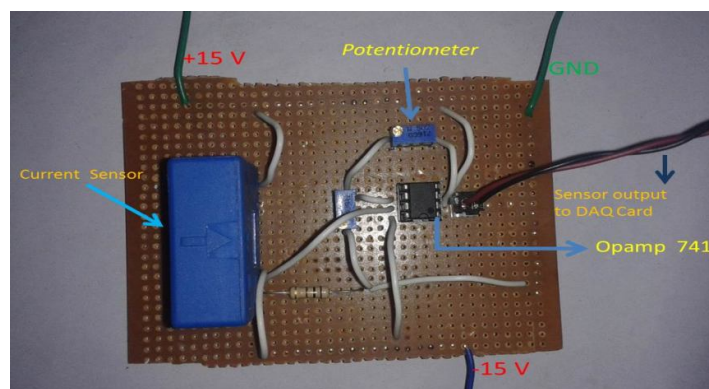


Fig.5.8 Current sensor card

The number of secondary turns (N_s) is 1000 and the maximum value of secondary current (I_s) is 50mA. Primary current (I_p) is the current that is to be measured. The magnetic flux created by the primary current is balanced through a secondary coil using a Hall device and associated electronic circuit. The relation given by Equation (5.1) holds true during operation.

$$N_p \times I_p = N_s \times I_s \quad (5.1)$$

Where, N_p is number of primary turns. In the experiment, $N_p = 1$, thus a primary current up to 50A can be safely measured. Since the turn ratio is constant, the secondary current is an exact representation of the primary current. The output signal is the voltage drop on the resistance R_m caused by the secondary current. A 100Ω resistance is selected as R_m . This output signal needs to be scaled within the analog input limits (-10V to +10V) of data acquisition card, which is done by a non-inverting opamp configuration. Two variable resistances, R_i and R_f , are used to select a proper gain. The current sensor and opamp both require $\pm 15V$ supply for their operation which is provided by DC power supply module. The complete circuit is shown in Fig.5.7. It is then calibrated to find the exact relation between input current and output voltage. Two current sensor cards are required for sensing

1. Source current
2. Load current

Current sensor card for measuring source current

Current sensor card for source current measurement is designed for measuring alternating current of maximum of 10A (r.m.s). The sensor is calibrated such that sensor output is 2V for 1A of input current to be sensed. The curve fitting formula for current sensor card for measuring panel voltage is computed using MATLAB as

$$v_{out} = 2.189 \times i_{source} - 0.1207 \quad (5.2)$$

Current sensor card for measuring load current

Current sensor card for source load measurement was designed for measuring alternating current of maximum of 40A (r.m.s). The sensor is calibrated such that sensor output is 1V for 2A of input current to be sensed. The curve fitting formula for current sensor card for measuring panel voltage is computed using MATLAB as

$$v_{out} = 2.192 \times i_{load} + 0.1081 \quad (5.3)$$

The curve obtained from curve fitting tool of MATLAB for calibrating the current sensor (source) is shown in the Fig.5.9.

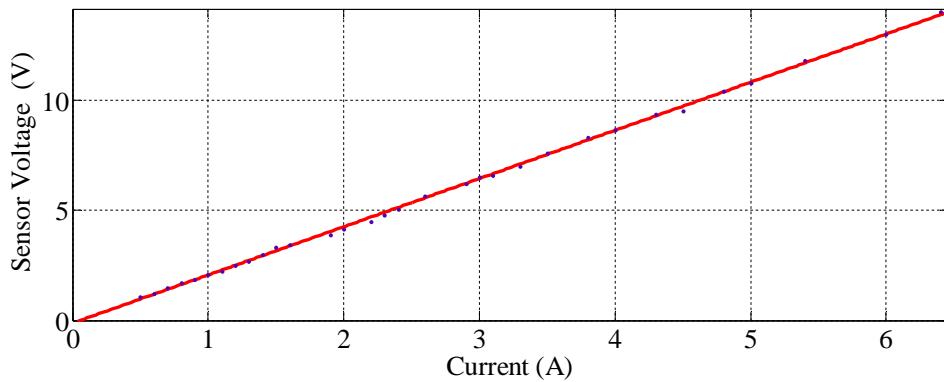


Fig.5.9 Linear relationship between sensor output voltage and input current

5.1.4.2 Voltage Sensor

Source voltage, load voltage dc-link capacitor voltages are to be sensed accurately for proper operation of controller. Three LEM manufactured voltage transducer LV 25-P are used to sense respective voltages. The complete specification of voltage sensor is provided in Appendix A. The design note for voltage sensor card and calibrations for acquiring correct sensed voltages are given in Appendix B. The voltage sensor card fabricated on printed circuit board is shown in Fig.5.10.

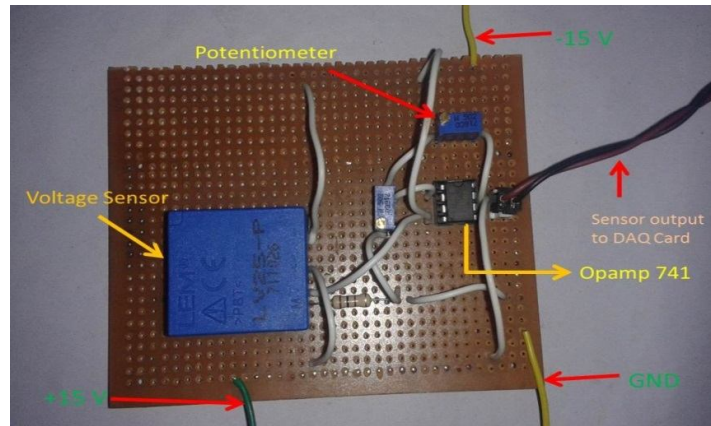


Fig.5.10 Voltage sensor card

The voltage sensor used is Hall Effect based voltage transducer. it can measure up to $\pm 500\text{V}$.

The primary current generated from primary voltage and a external resistor R_{in} creates primary magnetic flux. The magnetic flux is connected to the magnetic circuit. The hall device in the air gapped magnetic core provides a proportionate voltage to magnetic flux. This voltage and associated electronic circuit are used to generate the secondary (compensating) current that is an exact representation of the primary voltage. The secondary current is passed through measuring resistance R_m . The voltage drop across R_m is provided to op-amp LM741, operated in non-inverting mode to scale the sensor output signal to a range suitable for ADC pins i.e. 0-10 V. The voltage sensor and op-amp both require $\pm 15\text{V}$ supply for their operation which is provided by a DC power supply module. The specification of LV-25P transducer is given in Appendix B

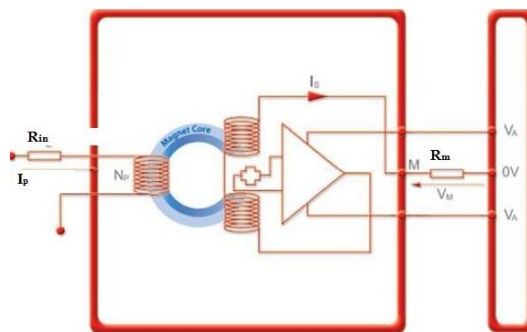


Fig.5.11 Working principle of voltage sensor

Three voltage sensor cards are required for sensing:

1. Source voltage
2. Load voltage
3. DC link capacitor voltage

All three voltage sensor card for were designed for measuring maximum of 500V (470V).

The value of input resistance placed at the positive terminal of voltage transducer considering optimum accuracy at nominal primary current of 10mA, was $50\text{K}\Omega/5\text{W}$. A resistance of $65\text{K}\Omega/5\text{W}$ was placed. The sensor is calibrated such that sensor output is 1V for 10V of input voltage to be sensed. The curve fitting formulas for three voltage sensors are computed as:

$$\text{For source voltage sensor, } v_{out} = 0.0923 \times v_{source} + 0.2380 \quad (5.4)$$

$$\text{For load voltage sensor, } v_{out} = 0.0904 \times v_{load} + 0.2541 \quad (5.5)$$

$$\text{For DC link voltage sensor, } v_{out} = 0.0941 \times v_{DC_link} + 0.3541 \quad (5.6)$$

The curve obtained from curve fitting tool of MATLAB for calibrating the voltage sensor (load) is shown in the Fig.5.12.

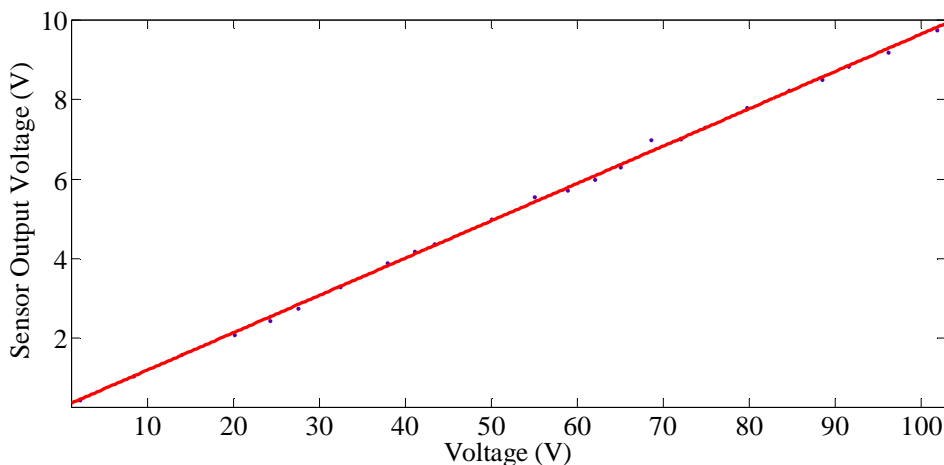


Fig.5.12 Linear relationship between sensor output voltage and input current

5.1.4.3 Gate Driver

High performance FUJI's hybrid IGBT driver IC, VLA517-01R will be used to provide the necessary driving signals to the IGBT across the gate emitter terminals. This hybrid IC is a circuit designed for driving n-channel IGBT modules. An optocoupler is used in this chip to provide the required isolation between the signal side of the chip and the power side. The input to the chip is a digital signal of +5V as logic high and 0V as logic low and the corresponding outputs are +15V and -5V which is shown in Fig.5.13.

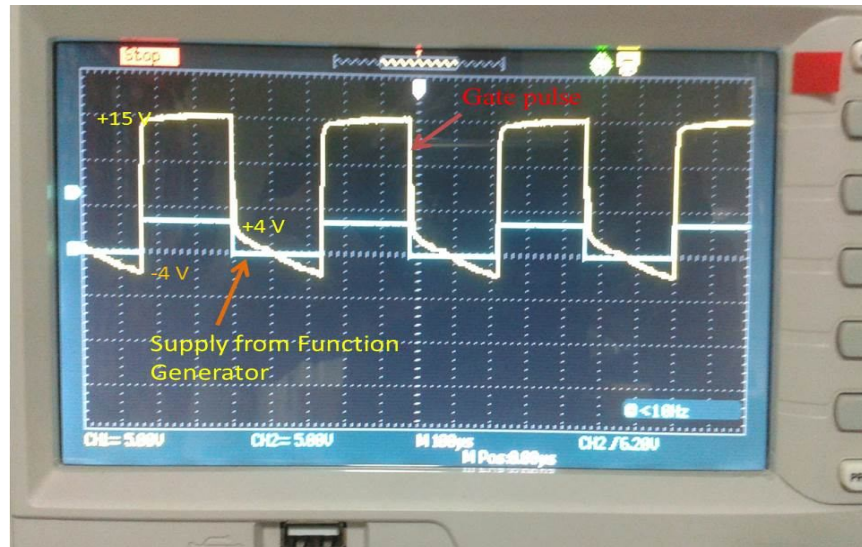


Fig.5.13 Gate driver output

Output of this chip is connected through a proper gate series resistance ($R_g=25\Omega$) across the gate emitter terminals of the corresponding IGBT, which is to be driven. The input logic signal given to the chip should be capable of driving a current of 10mA for the satisfactory operation of this chip. The pin description and details of the IC VLA517-01R are given in the Appendix C. The circuit diagram implemented in the present work for the IGBT driver is shown in Fig.5.14. The complete gate driver circuit is fabricated and is shown in Fig.5.15.

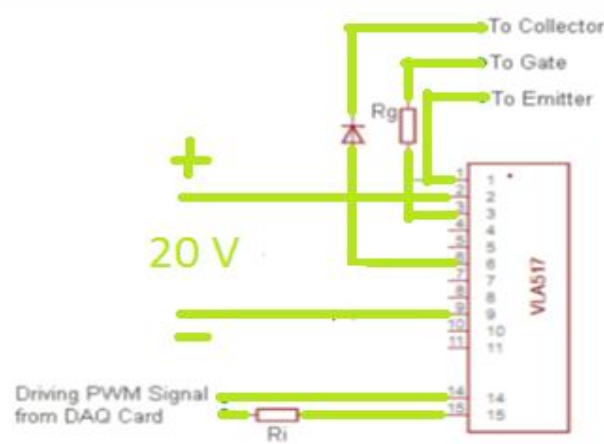


Fig.5.14 Schematics of gate driver circuit

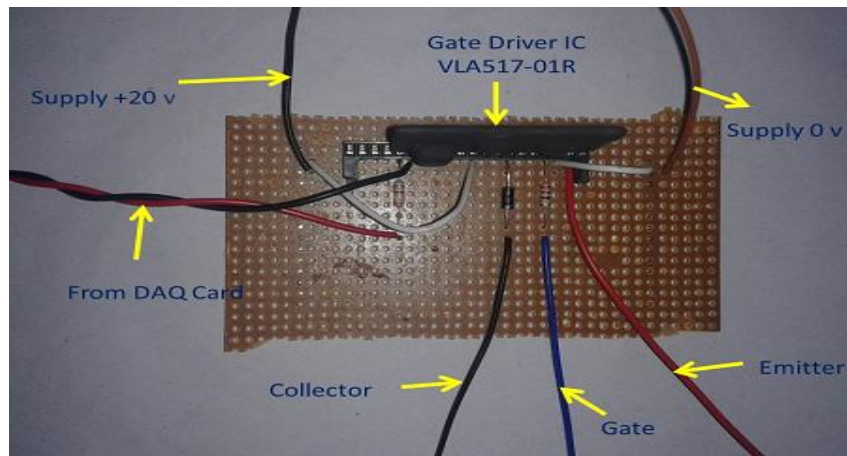


Fig.5.15 Gate driver card

5.1.6 Filter Inductor

The purpose of using filter inductor is to eliminate very high frequency component from filter injected current and to limit the inrush current to protect IGBT .

CHAPTER 6

Conclusion and Future Activity

6.1 CONCLUSION

From MATLAB/SIMULINK simulation of hysteresis current controller based active power filter, it is found that THD of source current is reduced to 1.86 % from 29.86 % after use of filter. Reactive power required by nonlinear load is completely compensated by active power filter (APF) and power factor at source end becomes almost unity. By using triangular carrier current controller based active power filter, it is found that THD of source current is reduced to 3.64 % from 29.38 % and reactive power is also completely compensated and power factor is also found to be unity at the source end. The higher THD value in compensated source current of triangular carrier current controller based active power filter is due to low switching frequency of carrier wave which I cannot increase beyond 10 KHz due to computational limitation of my computer.

Due to late delivery of some components and lack of availability of proper interfacing devices at the last moment, I could not able to run the complete setup to validate the simulation result. In future I will try to validate the simulation works through experimentation.

REFERENCES:

- [1] Grady, W. Mack, and Surya Santoso. "Understanding power system harmonics." *IEEE Power Engineering Review* 21.11 (2001): 8-11.
- [2] Morán, Luis A., et al. "Using active power filters to improve power quality." *5th Brazilian Power Electronics Conference*. 1999.
- [3] Jou, H-L. "Performance comparison of the three-phase active-power-filter algorithms." *IEE Proceedings-generation, Transmission and Distribution* 142.6 (1995): 646-652.
- [4] Chin Chen, Chin-Lin, and Chin E. Lin. "An active filter for an unbalanced three-phase system using the synchronous detection method." *Electric power systems research* 36.3 (1996): 157-161.
- [5] Rashid, Muhammad H. "Power electronics handbook, 2007."
- [6] Seifossadat, S. G., et al. "Quality improvement of shunt active power filter, using optimized tuned harmonic passive filters." *Power Electronics, Electrical Drives, Automation and Motion, 2008. SPEEDAM 2008. International Symposium on*. IEEE, 2008.
- [7] B Singh, Ambrish Chandra, Kamal Al-Haddad, Bhim. "Computer-aided modeling and simulation of active power filters." *Electric Machines &Power Systems* 27.11 (1999): 1227-1241.
- [8] Henderson, Robert D., and Patrick J. Rose. "Harmonics: the effects on power quality and transformers." *Industry Applications, IEEE Transactions on* 30.3 (1994): 528-532.
- [9] Dahono, P. A. "New hysteresis current controller for single-phase full-bridge inverters." *Power Electronics, IET* 2.5 (2009): 585-594.
- [10] Prusty, Smruti. *FPGA Based Active Power Filter for Harmonics Mitigation*. Diss. 2011.

Appendix A:

LEM Current Transducer (LA 55-P)

Table A1. Specification of Current Sensor

Electrical data					
I_{PN}	Primary nominal r.m.s. current	50		A	
I_p	Primary current, measuring range	0 .. ± 70		A	
R_M	Measuring resistance @	$T_A = 70^\circ\text{C}$	$T_A = 85^\circ\text{C}$	$R_{M\min}$	$R_{M\max}$
		$R_{M\min}$	$R_{M\max}$	$R_{M\min}$	$R_{M\max}$
	with ± 12 V	@ ± 50 A _{max}	10 100	60 95	Ω
		@ ± 70 A _{max}	10 50	60 ¹⁾ 60 ¹⁾	Ω
	with ± 15 V	@ ± 50 A _{max}	50 160	135 155	Ω
		@ ± 70 A _{max}	50 90	135 ²⁾ 135 ²⁾	Ω
I_{SN}	Secondary nominal r.m.s. current	50		mA	
K_N	Conversion ratio	1 : 1000			
V_c	Supply voltage (± 5 %)	± 12 .. 15		V	
I_c	Current consumption	10 (@± 15 V) + I_s		mA	
V_d	R.m.s. voltage for AC isolation test, 50 Hz, 1 mn	2.5		kV	
Accuracy - Dynamic performance data					
X	Accuracy @ I_{PN} , $T_A = 25^\circ\text{C}$	$\pm 15 \text{ V} (\pm 5 \%)$	± 0.65	%	
		$\pm 12 .. 15 \text{ V} (\pm 5 \%)$	± 0.90	%	
ϵ_L	Linearity	< 0.15		%	
I_o	Offset current @ $I_p = 0$, $T_A = 25^\circ\text{C}$			Typ	Max
I_{DM}	Residual current ³⁾ @ $I_p = 0$, after an overload of $3 \times I_{PN}$			± 0.2	mA
I_{OT}	Thermal drift of I_o	$0^\circ\text{C} .. + 70^\circ\text{C}$	± 0.1	± 0.5	mA
		$-25^\circ\text{C} .. + 85^\circ\text{C}$	± 0.1	± 0.6	mA
t_a	Reaction time @ 10 % of $I_{P\max}$	< 500		ns	
t_r	Response time @ 90 % of $I_{P\max}$	< 1		μs	
di/dt	di/dt accurately followed	> 200		A/μs	
f	Frequency bandwidth (- 1 dB)	DC .. 200		kHz	
General data					
T_A	Ambient operating temperature	- 25 .. + 85		°C	
T_s	Ambient storage temperature	- 40 .. + 90		°C	
R_s	Secondary coil resistance @	$T_A = 70^\circ\text{C}$	80	Ω	
		$T_A = 85^\circ\text{C}$	85	Ω	
m	Mass	18		g	
	Standards ⁴⁾	EN 50178			

Appendix B:

LEM Voltage Transducer (LV 25-P)

Table B1. Specification of Voltage Sensor

Electrical data				
I_{PN}	Primary nominal current rms	10		mA
I_{PM}	Primary current, measuring range	0 .. ± 14		mA
R_M	Measuring resistance	$R_{M\min}$	$R_{M\max}$	
	with ± 12 V	@ ± 10 mA _{max}	30	190
		@ ± 14 mA _{max}	30	100
	with ± 15 V	@ ± 10 mA _{max}	100	350
		@ ± 14 mA _{max}	100	190
I_{SN}	Secondary nominal current rms	25		mA
K_N	Conversion ratio	2500 : 1000		
V_C	Supply voltage (± 5 %)	± 12 .. 15		V
I_C	Current consumption	10 (@ ± 15 V) + I_S		mA
Accuracy - Dynamic performance data				
X_G	Overall accuracy @ I_{PN} , $T_A = 25^\circ C$ @ ± 12 .. 15 V @ ± 15 V (± 5 %)	± 0.9		%
ε_L	Linearity error	< 0.2		%
I_O	Offset current @ $I_P = 0$, $T_A = 25^\circ C$		Typ	Max
I_{OT}	Temperature variation of I_O	0°C .. + 25°C	± 0.06	± 0.15
		+ 25°C .. + 70°C	± 0.10	± 0.25
t_r	Response time ¹⁾ to 90 % of I_{PN} step	40		μs
General data				
T_A	Ambient operating temperature	0 .. + 70		°C
T_s	Ambient storage temperature	- 25 .. + 85		°C
R_p	Primary coil resistance	@ $T_A = 70^\circ C$	250	Ω
R_s	Secondary coil resistance	@ $T_A = 70^\circ C$	110	Ω
m	Mass	22		g
	Standard	EN 50178: 1997		

Appendix C:

VLA517-01R Hybrid IC for Driving IGBT Modules

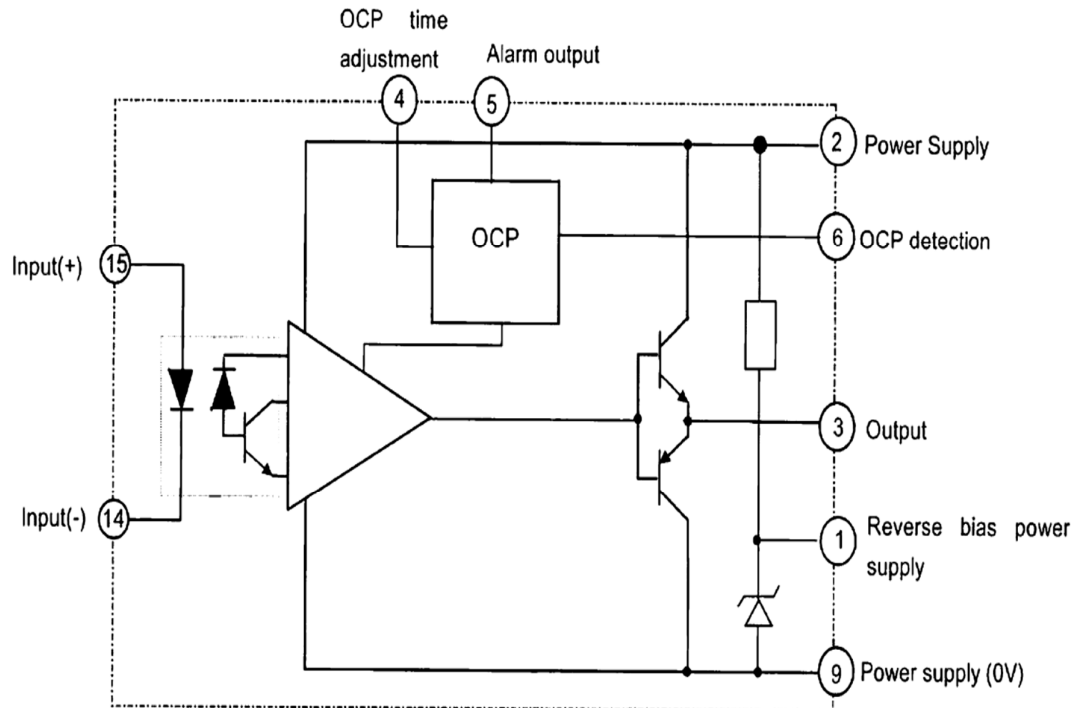


Fig.C1 Pin description of IC

Appendix D:

Semikron IGBT Module (SKM 75GB063D)

Table D1. Characteristics of the IGBT Module

Absolute Maximum Ratings		$T_c = 25^\circ\text{C}$, unless otherwise specified		
Symbol	Conditions	Values		Units
IGBT				
V_{CES}		600		V
I_C	$T_c = 25 \text{ (75)}^\circ\text{C}$	100 (75)		A
I_{CRM}	$t_p = 1 \text{ ms}$	150		A
V_{GES}		± 20		V
$T_{vj} \text{ (T}_{\text{sg})}$	$T_{\text{OPERATION}} \leq T_{\text{sg}}$	- 40 ... + (125) 150		°C
V_{isol}	AC, 1 min.	2500		V
Inverse diode				
I_F	$T_c = 25 \text{ (80)}^\circ\text{C}$	75 (50)		A
I_{FRM}	$t_p = 1 \text{ ms}$	150		A
I_{FSM}	$t_p = 10 \text{ ms; sin.; } T_j = 150^\circ\text{C}$	440		A
Freewheeling diode				
I_F	$T_c = 25 \text{ (80)}^\circ\text{C}$	100 (75)		A
I_{FRM}	$t_p = 1 \text{ ms}$	200		A
I_{FSM}	$t_p = 10 \text{ ms; sin.; } T_j = 150^\circ\text{C}$	720		A
Characteristics		$T_c = 25^\circ\text{C}$, unless otherwise specified		
Symbol	Conditions	min.	typ.	max.
IGBT				
$V_{GE(\text{th})}$	$V_{GE} = V_{CE}, I_C = 1 \text{ mA}$	4,5	5,5	6,5
I_{CES}	$V_{GE} = 0, V_{CE} = V_{CES}, T_j = 25 \text{ (125)}^\circ\text{C}$	0,1	0,3	mA
$V_{CE(\text{TO})}$	$T_j = 25 \text{ (125)}^\circ\text{C}$	1,05 (1)		V
r_{CE}	$V_{GE} = 15 \text{ V}, T_j = 25 \text{ (125)}^\circ\text{C}$	14 (18,7)		mΩ
$V_{CE(\text{sat})}$	$I_{Cnom} = 75 \text{ A}, V_{GE} = 15 \text{ V, chip level}$	2,1 (2,4)	2,5 (2,8)	V
C_{ios}	under following conditions	4,2		nF
C_{oes}	$V_{GE} = 0, V_{CE} = 25 \text{ V, f} = 1 \text{ MHz}$	0,5		nF
C_{res}		0,3		nF
L_{CE}			30	nH
$R_{CC+EE'}$	res., terminal-chip $T_c = 25 \text{ (125)}^\circ\text{C}$	0,75 (1)		mΩ
$t_{d(on)}$	$V_{CC} = 300 \text{ V, } I_{Cnom} = 75 \text{ A}$	60		ns
t_r	$R_{Gon} = R_{Goff} = 15 \Omega, T_j = 125^\circ\text{C}$	50		ns
$t_{d(off)}$	$V_{GE} = \pm 15 \text{ V}$	350		ns
t_f		35		ns
$E_{on} (E_{off})$		3 (2,5)		mJ
Inverse diode				
$V_F = V_{EC}$	$I_{Fnom} = 75 \text{ A; } V_{GE} = 0 \text{ V; } T_j = 25 \text{ (125)}^\circ\text{C}$	1,55 (1,55)	1,9	V
$V_{(TO)}$	$T_j = 125 \text{ () }^\circ\text{C}$	0,9		V
r_T	$T_j = 125 \text{ () }^\circ\text{C}$	10	13,3	mΩ
I_{RRM}	$I_{Fnom} = 75 \text{ A; } T_j = 125 \text{ () }^\circ\text{C}$	30		A
Q_{rr}	$dV/dt = 800 \text{ A}/\mu\text{s}$	3,7		μC
E_{rr}	$V_{GE} = 0 \text{ V}$			mJ
FWD				
$V_F = V_{EC}$	$I_F = 100 \text{ A; } V_{GE} = 0 \text{ V, } T_j = 25 \text{ (125)}^\circ\text{C}$	1,55 (1,55)	1,9	V
$V_{(TO)}$	$T_j = 125 \text{ () }^\circ\text{C}$	0,9		V
r_T	$T_j = 125 \text{ () }^\circ\text{C}$	8	10	mΩ
I_{RRM}	$I_F = 100 \text{ A; } T_j = 125 \text{ () }^\circ\text{C}$	44		A
Q_{rr}	$dV/dt = 0 \text{ A}/\mu\text{s}$	6		μC
E_{rr}	$V_{GE} = V$			mJ
Thermal characteristics				
$R_{th(j-c)}$	per IGBT		0,35	K/W
$R_{th(j-c)D}$	per Inverse Diode		1	K/W
$R_{th(j-c)FD}$	per FWD		0,6	K/W
$R_{th(c-s)}$	per module		0,05	K/W
Mechanical data				
M_s	to heatsink M6	3	5	Nm
M_t	to terminals M5	2,5	5	Nm
w			160	g